SLAC PUB 4581
March 1988
(N)

THE ELECTRON SPECTRUM FROM B MESON DECAYS

THE CRYSTAL BALL COLLABORATION

K. Wachs[4], D. Antreasyan[8], H.W. Bartels[4], Ch. Bieler[7], J.K. Bienlein[4], A. Bizzeti[6], E.D. Bloom[10], K. Brockmüller[4], A. Cartacci[6], M. Cavalli-Sforza[2], R. Clare[10], A. Compagnucci[6], G. Conforto[6], S. Cooper[a,11], D. Coyne[2], G. Drews[4], K. Fairfield[10], G. Folger[5], A. Fridman[b,11], D. Gelphman[10], G. Glaser[5], G. Godfrey[10], K. Graaf[7], F.H. Heimlich[7], F.H. Heinsius[7], R. Hofstadter[10], J. Irion[8], Z. Jakubowski[3], K. Karch[11], S. Keh[11], T. Kiel[7], H. Kilian[11], I. Kirkbride[10], M. Kobel[5], W. Koch[4], A.C. König[9], K. Königsmann[11], S. Krüger[7], G. Landi[6], S. Leffler[10], R. Lekebusch[7], A.M. Litke[10], S. Lowe[10], B. Lurz[5], H. Marsiske[4], W. Maschmann[7], P. McBride[8], H. Meyer[4], B. Muryn[3], W.J. Metzger[9], B. Monteleoni[6], B. Niczyporuk[10], G. Nowak[3], C. Peck[1], C. Pegel[7], P.G. Pelfer[6], F.C. Porter[1], M. Reidenbach[8], M. Scheer[11], P. Schmitt[11], J. Schotanus[9], J. Schütte[8], A. Schwarz[10], F. Selonke[4], D. Sievers[7], T. Skwarnicki[4], V. Stock[7], K. Strauch[8], U. Strohbusch[7], J. Tompkins[10], B. van Uitert[10], R.T. Van de Walle[9], A. Voigt[4], U. Volland[5], K. Wacker[10], W. Walk[8], H. Wegener[5], D. Williams[8]

[1] *California Institute of Technology, Pasadena, CA 91125, USA*
[2] *University of California at Santa Cruz, Santa Cruz, CA 95064, USA*
[3] *Cracow Institute of Nuclear Physics, PL-30055 Cracow, Poland*
[4] *Deutsches Elektronen Synchrotron DESY, D-2000 Hamburg, Germany*
[5] *Universität Erlangen-Nürnberg, D-8520 Erlangen, Germany*
[6] *INFN and University of Firenze, I-50100 Firenze, Italy*
[7] *Universität Hamburg, I. Institut für Experimentalphysik, D-2000 Hamburg, Germany*
[8] *Harvard University, Cambridge, MA 02138, USA*
[9] *University of Nijmegen and NIKHEF NL-6525 ED Nijmegen, The Netherlands*
[10] *Department of Physics, HEPL, and Stanford Linear Accelerator Center, Stanford University, Stanford, CA 94305, USA*
[11] *Universität Würzburg, D-8700 Würzburg, Germany*

Abstract. The Crystal Ball collaboration has measured the energy spectrum of electrons from semileptonic B meson decays at the e^+e^- - storage ring DORIS II. Branching ratios and semileptonic widths have been measured using several models for the hadronic matrix elements. The branching ratio for semileptonic B meson decays into charmed states X_c has been found to be $BR(B \to e\nu X_c) = (11.7 \pm 0.4 \pm 0.7)\%$ as an average of all models used. The average result for the Kobayashi - Maskawa matrix element is $|V_{cb}| = 0.052 \pm 0.005 \pm 0.005$. Upper limits on $|V_{ub}/V_{cb}|$ have been obtained. The weakest upper limit, $|V_{ub}/V_{cb}| < 0.26$ is obtained using the model by Grinstein *et al.* with data of electron energy $E_e > 2.4$ GeV. Using models by Altarelli *et al.*, Wirbel *et al.*, and Körner *et al.* one gets an upper limit of $|V_{ub}/V_{cb}| < 0.15$.

---

[a] Present Address: Massachusetts Institute of Technology, Cambridge, MA 02139, USA

[b] Permanent Address: DPHPE, Centre d'Etudes Nucléaires de Saclay, F-91191 Gif sur Yvette, France

Printed in the Zeitschrift fur Physik C42:33 1989

1. Introduction

The $\Upsilon(4S)$ resonance is an ideal system to study weak b flavoured decays. The resonance lies above the open B meson threshold and therefore decays entirely into $B\overline{B}$ meson pairs [1]. A b quark in the B meson decays either into a c or a u quark emitting a virtual W^- boson, which then can weakly disintegrate into an electron and its antineutrino. The mass and spin of the final state meson influence the transition probability and the shape of the electron spectrum. Due to the heavier c quark mass compared to that of the u quark, non-charmed mesons (X_u) are in general lighter than charmed mesons (X_c). Hence the electron spectrum originating from B meson decays to non-charmed mesons extends to higher energies and this difference can therefore be used to measure the transition $b \to u$. Several models predict the partial width and the shape of the electron spectrum of the $B \to e\nu X_c$ and $B \to e\nu X_u$ transitions. We measure the electron spectrum from $\Upsilon(4S)$ decays,

$$e^+e^- \to \Upsilon(4S) \to \begin{array}{ll} B\overline{B} & \\ B \to & e\,X \end{array} \qquad (1)$$

and then fit the data to the assumption that the spectrum consists of a $b \to c$, a $b \to u$, and a $c \to s$ (from subsequent decays of charmed particles) contribution. Those contributions are converted to branching ratios and are used to measure the Kobayashi - Maskawa matrix elements. The $\Upsilon(4S)$ resonance is produced on top of a large continuum - see figure 1. We use two data samples one "ON" $\Upsilon(4S)$ and the other one in the continuum below the $\Upsilon(4S)$ resonsance for background subtraction. In addition the background from particles faking electrons from

$$\Upsilon(4S) \to B\overline{B} \to hadrons$$

is investigated. The paper is therefore divided into the following subparts. After this introduction we first discuss the theoretical models of B meson decays, their predictions for the electron spectrum and their impact on the analysis. Then the Crystal Ball detector is described. Chapter four explains the data analysis. In chapters 5, 6, and 7 we disscuss the results for $(b \to u)/(b \to c)$ and for the branching ratio $BR(B \to e\nu X_c)$ and the systematic errors, respectively. In the last part these measurements are compared to previous results from other experiments. Moore details of the analysis can be found in [2].

2. Predictions for the Electron Spectrum from B Meson Decays

In order to extract branching ratios and widths from the measured electron spectrum, we need theoretical predictions for the shapes of the $b \to c$ and $b \to u$ spectra. We write the electron spectrum as $d\Gamma/dE_e$, where Γ is the partial width of the decay $B \to e\nu X$. The differential energy spectrum $d\Gamma/dE_e$ depends on the spin and mass of the individual final states in the charmed channels X_c^i ($i = D, D^* ...$) and the u quark channels X_u^j ($j = \pi, \rho ...$) and on the Kobayashi - Maskawa matrix elements [3] V_{cb} and V_{ub}. It can be written as

$$\frac{d\Gamma(B \to e\nu X)}{dE_e} = |V_{cb}|^2 \sum_i \frac{d\hat{\Gamma}(B \to e\nu X_c^i)}{dE_e} + |V_{ub}|^2 \sum_j \frac{d\hat{\Gamma}(B \to e\nu X_u^j)}{dE_e} . \qquad (2)$$

The spectra $d\hat{\Gamma}(B \to e\nu X)/dE_e$ can be calculated using models for the weak matrix elements between the B meson and the individual final state mesons. The Kobayashi - Maskawa matrix elements $|V_{cb}|$ and $|V_{ub}|$ are free parameters in the model and have to be measured by the experiment. The weak matrix elements have been calculated by several approaches: Altarelli, Cabibbo, Corbo, Maiani and Martinelli (ACM) [4] modified the free quark decay by considering a spectator quark and gluonic corrections. Grinstein, Isgur and Wise (GIW) [5], Wirbel, Stech and Bauer (WSB) [6], Köner and Schuler (KS) [7] and Pietschmann and Schöberl (PS) [8] use either non-relativistic or relativistic calculations to get the matrix elements of the weak hadronic current.

2.1 Free Quark Spectator Model

To start the description of the weak decay of B mesons we first briefly describe the decay of free quarks [4]. Here the light quark in the B meson is regarded as a mere spectator and the B meson decay is approximated as the decay of a free b quark into $e\nu c$ or $e\nu u$. This model predicts for the electron spectrum of $b \to e\nu c$

$$\frac{d\Gamma_{cb}^{f.q.}}{dx} = |V_{cb}|^2 \times \frac{d\hat{\Gamma}(b \to e\nu c)}{dx} = |V_{cb}|^2 \times \frac{G_F^2 m_b^5}{96\pi^3} \times g(z,x) \qquad (3)$$

with $g(z,x) = \frac{x^2[1 - z^2 - x]\,[(1 - x)(3 - 2x) + (3 - x)z^2]}{(1 - x)^3}$

and $z = m_c/m_b$, $x = E_e/m_b$ where m_c (m_b) denote the c (b) quark masses, respectively. They are free parameters in this model.

The shape of $d\Gamma/dE_e$ may be significantly changed by effects ignored in the free

quark model. However, the total semileptonic width Γ calculated in this model is expected to be reliable [5]. Integrating equation (3) over x yields

$$\Gamma_{cb} \equiv |V_{cb}|^2 \hat{\Gamma}^{f.q.}(b \to c\nu c) = |V_{cb}|^2 \times \frac{G_F^2 m_b^5}{192\pi^3} \times f(z) \qquad (4)$$

with $f(z) = 1 - 8z^2 + 8z^6 - z^8 - 24z^4 \ln z$.
Replacing c by u in equations (3) and (4) gives the results for the $b \to u$ transition.

2.2 Modified Free Quark Spectator Model

Atarelli, Cabibbo, Corbo, Maiani and Martinelli (ACM) [4] have modified the free quark spectator model to include effects of binding the b quark inside the B meson. The b quark is assumed to be moving with momentum $\vec{p}$ inside the meson, where p is distributed according to a Maxwell distribution :

$$\frac{dN(|\vec{p}|)}{d|\vec{p}|} = \frac{4\ |\vec{p}|^2}{\sqrt{\pi}\ p_F^3} \exp\left(-\frac{|\vec{p}|^2}{p_F^2}\right), \qquad (5)$$

with an adjustable Fermi motion parameter p_F. Together with the spectator quark the b quark forms the B meson of mass M_B. Energy and momentum conservation yields for the effective b quark mass

$$m_b^2 = M_B^2 + m_{sp}^2 - 2M_B\sqrt{|\vec{p}|^2 + m_{sp}^2} \qquad (6)$$

where m_{sp} is the mass of the spectator quark. $|\vec{p}|$ is constrained to a region where $m_b^2 > m_c^2$. As the term $M_B^2 = (5.280\,GeV/c^2)^2$ [9] is much bigger than the mass of the spectator $m_{sp}^2 \sim (0.15\,GeV/c^2)^2$, a variation of this m_{sp} contribution can be neglected. A variation of the spectator mass in the argument of the root can be absorbed in an effective change of the average momentum p_F. Hence the theory has the three free parameters m_c, m_u, p_F. The B meson mass is taken from other measurements [9]. The electron spectrum in the $\Upsilon(4S)$ center of mass system is obtained by boosting the spectrum (3) with momentum $|\vec{p}|$ of the b quark *and* the momentum of the B meson ($P_B \sim 0.325\ GeV/c$ or $\beta \sim 0.06$[9]). In addition the model takes into account the effect of soft gluon radiation. This correction can be written as: $Q(z,x) \sim 1 - 2\alpha_s G(z,x)/3\pi$. It has to be multiplied with Equations (3) and (4). For non-zero quark masses ($z \neq 0$) G depends only weakly on x and can be integrated independantly of equation(3): $G'(z) = \int G(z,x)dx$. G' is tabulated in the literature [10]. With the quark masses $m_c = 1.60\ GeV/c^2$, $m_b = 4.85\ GeV/c^2$, $m_u = 0.15\ GeV/c^2$ and the strong coupling constant $\alpha_s = 0.24$ one obtaines for the gluonic correction: $Q(z = 1.60/4.85) = 0.88$ in the $b \to c$ channel and $Q(z = 0.15/4.85) = 0.82$ in the $b \to u$ channel.

2.3 Non- relativistic Constituent Quark Model

In general the electron spectrum of the weak decay $B^{\frac{+}{0}} \rightarrow e^{\frac{+}{+}} \bar{\nu}_e X^{\frac{0}{-+}}$ can be written (neglecting the effect of the electron mass) as:

$$\frac{d^2\hat{\Gamma}}{dx\,dy} \propto \frac{G_F^2 M_B^5}{32\pi^3} \times \left(\frac{\alpha}{M_B^2} y + 2\beta\left[2x(1 - \frac{M_X^2}{M_B^2} + y) - 4x^2 - y\right] - \gamma y\left[1 - \frac{M_X^2}{M_B^2} - 4x + y\right]\right) \quad (7)$$

with $x = E_e/M_B$, $y = (P_B - P_X)^2/M_B^2$ and $P_B, M_B; P_X, M_X$ denoting the 4-momenta and the masses of initial and final state mesons, respectively. The form factors α, β and γ have to be calculated for the individual decays. This is done by GIW[5] using a non relativistic constituent quark model. Harmonic oscillator wave functions are used to calculate the meson wave functions with a 'Coulomb plus linear' $q-\bar{q}$ potential ansatz. The form factors α, β, γ are calculated for the transitions to final state mesons with $1S, 1P, 2S$ quantum states. The calculated transition rates ($B \rightarrow D, D^*, D^{**}$) saturate the free quark prediction in the case of $b \rightarrow c$, where the transitions to D, D^* account for $\simeq 90\%$ of the calculated rate. For $b \rightarrow u$, mass states up to 1.5 GeV/c^2 are taken into account. As higher mass states will contribute only to electron energies below $\simeq 2.2\ GeV$ the predicted inclusive electron energy spectrum is valid only above $\simeq 2.2\ GeV$. Hence we use the $b \rightarrow u$ prediction for the calculation of branching ratios and $|V_{ub}|$ only above $E_e - 2.2\ GeV$. Thus only

$$\frac{BR(B \rightarrow e\nu X(1S, 1P, 2S)_u)}{BR(B \rightarrow e\nu X(1S, 1P, 2S)_c)} \text{ instead of } \frac{BR(B \rightarrow e\nu X_u)}{BR(B \rightarrow e\nu X_c)}$$

is predicted.

2.3a Corrections to the non - relativistic Constituent Quark Model

Altomari and Wolfenstein (AW) [11] have modified GIW's model in the $b \rightarrow c$ channel. They treat the constituent quark masses slightly differently, but get quite similar numbers for the $B \rightarrow e\nu D$ channel (table 1). In the $B \rightarrow e\nu D^*$ channel they have tested the dependence of the semileptonic width as function of 'a_+', a factor appearing in the calculation of the formfactor β. It was set to 0 by GIW. With AW's preferred value for 'a_+' the semileptonic width $\Gamma(B \rightarrow e\nu D^*)$ becomes smaller by a factor of 1.78 compared to the prediction by GIW.

2.4 Relativistic Bound State Model I

The third model, by WSB [6], uses relativistic bound state wave functions to calculate the rates. Form factors are calculated in the infinite momentum frame at $q^2 = 0$, i.e. at the electron endpoint. The quantity q^2 in WSB's model is called $y \times M_B^2$ in the paper by GIW. The form factors are extrapolated to $q^2 \neq 0$ under the assumption of nearest pole dominance. Only transitions to the $1S$ final states D, D^* and π, ρ, respectively, have been calculated. Following the arguments discussed above, this implies a lower fit limit of $E_e \simeq 1.7\ GeV$ for the $b \to c$ transitions and $E_e \simeq 2.3\ GeV$ for $b \to u$. Only

$$\frac{BR(B \to e\nu\pi, \rho)}{BR(B \to e\nu D, D^*)} \text{ instead of } \frac{BR(B \to e\nu X_u)}{BR(B \to e\nu X_c)}$$

is predicted.

2.5 Relativistic Bound State Model II

The fourth model discussed now, by Körner and Schuler (KS) [7], uses in principle the same ansatz as WSB, but take dipol formfactors for the calculation of the decay into D^* and ρ mesons. Similar quantities like the overlap factor of the initial and final state meson are used. The valididty limits for the prediction of the inclusive electrons spectrum are the same as quoted for WSB.

2.6 Non Relativistic Scalar + Vector $q\bar{q}$ Potential

The last model is proposed by Pietschmann and Schöberl (PS) [8] The parameters of their quark potential model, were the potential consists out of a scalar and a vector part, were tuned to fit the charmonium and bottonium states. Since we already find serious discrepancies between the data and the prediction the $b \to c$ channel, we cannot evaluate meaningful $(b \to u)/(b \to c)$ ratios with this model. Therefore we neither describe nor use their $b \to u$ prediction.

2.7 Comparison of Predictions

In table 1 the used parameters and predicted semileptonic widths are summarized. For the $b \to c$ channel the predictions agree quite well, if one applies the AW correction to the model by GIW. Figure 2 shows the $b \to c$ spectra normalized to 1 for ACM and GIW. The models by WSB, KS and PS have been normalized to 0.9 assuming, that the missing higher spin - and mass - states will contribute $\simeq 10\%$ to the decay. The shape of the contribution to the electron spectrum from

		Model					
		ACM	GIW	AW	WSB	KS	PS
m_b	$[GeV/c^2]$	$< 4.85 >$	5.120		4.900	4.900	5.240
m_c	$[GeV/c^2]$	1.607	1.820	1.800	1.700	1.700	1.850
$m_{u,d}$	$[GeV/c^2]$	0.150	0.330		0.350	0.350	0.340
$\Gamma_{cb} = \Gamma(B \to .)/(h\|V_{cb}\|^2)$	$10^{12}/sec$						
$B \to e\nu\, D$			11.0	12.3	8.1	8.3	7.2
$B \to e\nu\, D^*$			41.2	23.1	21.9	25.8	68.8
$B \to e\nu\,(D + D^*)$			52.2	34.1	30.0	34.1	76.0
$B \to e\nu\,(D + D^*) + 10\%$			57.4	38.9	33.0	37.5	83.6
$B \to e\nu\, X_c$		36.5	58.0				
$\Gamma_{ub} = \Gamma(B \to .)/(h\|V_{ub}\|^2)$	$10^{12}/sec$						
$B \to e\nu\, \pi$			2.0		7.4	7.25	
$B \to e\nu\, \rho$			16.0		26.1	33.0	
$B \to e\nu\,(\pi + \rho)$			18.0		33.5	40.25	
$B \to e\nu\, X(1S, 1P, 2S)_u$			57.0				
$B \to e\nu\, X_u$		75.9					

Table 1: Comparison of parameters and predicted semileptonic widths by the various models.

these channels is determined by the large masses of the mesons involved. Exept for the model by PS all predicted shapes essentially agree. The spectrum of the model by PS is much softer. The $b \to u$ spectra show a difference in shape and amplitude – see figure 2 and table 1. One reason for the different width in the meson decay models is the different treatment of the constituent quark masses in the models although the quark masses $m_{u,d}$ used are nearly identical. While GIW use the so called 'mock masses' $\tilde{m}$ - the sum of the constituent quark masses - for the meson masses, KS and WSB use the meson masses themselves for the calculation of the formfactors. Especially in the $B \to \pi$ channnel this choice has a major impact on the formfactor f (a and γ are zero for this decay). As β is proportional to $\exp(\ 1/\tilde{m}_\pi ...)$ in GIW's model, a choice of $\tilde{m}_\pi = 700$ or $140\ MeV$ easily explains the factor of 3 in the difference in the semileptonic width of the $B \to \pi$ transition. For the decay to a D meson the difference between the mock mass and the meson mass is much smaller and hence also the difference in the semileptonic width between the models.

In figure 2 also a prediction of the electron spectrum from subsequent $c \to s$ transitions is shown. This prediction is taken from the standard Lund string

fragmentation program 6.2 [12]. It is not well tested, because not all the $B \rightarrow X_e$ transitions have been measured in rate and X_e momentum distribution. But nevertheless it gives an approximation of the expected shape. As the main interest lies on the electrons from direct B meson decays we set the lower limit of the electron spectrum to be fully analyzed above 1.5 GeV. Using the data below $\approx$ 1 GeV would require a more accurate knowledge of the $c \rightarrow s$ transitions. The upper bound of the electron spectrum is set by a kinematical limit of the B meson decay. The B mesons are produced nearly at rest ($\beta = 0.06$). Hence the maximum momentum of particles coming from B meson decays is about $M_B/2 = 2.63\ GeV/c$. If one decay product has a non zero mass of e.g. 2.1 GeV/c^2 the maximum momentum reduces to 2.2 GeV. In this publication we do not measure $b \rightarrow u$ branching ratios, but ratios of branching ratios $(b \rightarrow u)/(b \rightarrow c)$. This has the advantage that the b quark (B meson) mass does not need to be known very precisely, as the term m_b^5 (M_B^5) in the semileptonic widths in (4 and 7) cancels for this ratio.

3. The Detector

The Crystal Ball detector [13] at the storage ring DORIS II at DESY has been used to measure the inclusive electron energy spectrum from B meson decays. The detector is shown in figure 3. It consists of 672 NaI(Tℓ) shower counters which detect photons and electrons with good spatial and energy resolution. Each shower counter has the shape of a truncated triangular pyramid pointing to the e^+e^- interaction point and is viewed by a phototube. The NaI counters form a sphere of 16 radiation lengths thickness (corresponding to about 1 nuclear interaction length) covering 93% of the 4π solid angle. Two holes are left for the beam pipe. The 60 crystals next to the beam pipe are called tunnel crystals. An additional 5% of 4π is covered by endcaps, consiting of 40 NaI(Tℓ) crystals. Electromagnetically showering particles deposit $\approx$ 98% of their energy in 13 adjacent crystals in a very symmetric pattern. Charged hadronic particles deposit very often only energy from minimum ionization, $\approx$ 200 MeV in one or two crystals. If a hadronic interaction takes place the deposited energy is much higher, but the pattern of the hadronic shower is very irregular. In the main ball (without endcaps) the energy resolution for electromagnetically showering particles is $\sigma_E/E = (2.7 \pm 0.2)\%/\sqrt[4]{E/GeV}$. The angular resolution varies with energy between $1^0 - 2^0$ for electromagnetically showering particles. A time of flight system located at the roof of the detector housing covers 25% of the solid angle. Together with a timing information from

the main ball it is used to detect cosmic muons. Charged particles are detected in a set of 800 proportional aluminum-tube wire chambers assembled in 4 cylindrical double layers around the beam pipe. The tubes are filled with a gas mixture of $79\%Ar + 20\%CO_2 + 1\%CH_4$ at a pressure of 1 bar. The tubes are parallel to the beam axis (z coordinate) and are $\simeq$ 64 cm long at a distance of 6.2 cm away from the beam axis (innermost layer) and $\simeq$ 37 cm long at a distance of 14.8 cm (outermost layer). The outer layer covers 77.8% of 4π solid angle. Charge division readout allows a determination of the z position of hits from electrons with an accuracy $\sigma_z \simeq 2$ cm / 0.6 cm in the inner / outer layers. In athimuthal direction a resolution per double layer of $\simeq$ 50 $mrad$ / 20 $mrad$ in the inner / outer double layers is achieved. The beam pipe has a thickness equivalent to 0.017 radiation lengths, each double layer has 0.01 r.l.

4. Data Analysis

The data samples used in this analysis are listed in table 2. The luminosity is obtained by measuring large angle Bhabha scattering in the main ball with a systematic accuracy of 2.5%[14,2]. The events satisfy our total energy trigger, which is fully efficient for events depositing at least 1.9 GeV in the NaI(Tℓ) crystals which lie within $|\cos\theta| < 0.85$.

	ON $\Upsilon(4S)$	continuum	$B\bar{B}$
Luminosity [pb $^{-1}$]	75.6	18.5	
observed hadronic events	288563	56720	$\approx$ 60000
produced hadronic events			$\approx$ 64000

Table 2: Data samples used

4.1 Event Selection

The selection for hadronic events has to remove background due to beam-gas and beam-wall interactions, cosmic rays, two photon induced events and QED, especially (radiative) Bhabha, events. The center of mass system of beam - gas and beam - wall interactions is boosted along the beam axis while for e^+e^- interactions the center of mass system is identical with the laboratory frame. Other than multihadronic events have mostly a smaller multiplicity. Those charactersistics are used to distinguish the event classes. In detail we do the following. We define the

energy seen in the 672 crystals in the main ball as $E_{BALL} = \sum_{i=1}^{672} E_i$ and a connected region ($\equiv CONREG$) as a group of adjacent crystals with energies greater than 10 MeV each. Hadronic events then have to pass the following selection criteria:

1. The first group of cuts suppresses QED events.
   We require a minimum multiplicity: There should be at least 3 energy clusters with an energy $E_{CONREG} > 100$ MeV each.
   If radiative Bhabhas have photons with more than 100 MeV the two following cuts reduce them further more: Events should have at most 1 energy cluster with $E_{CONREG} > 0.80\, E_{BEAM}$ and should not have any energy cluster with $E_{CONREG} > 0.80\, E_{BEAM}$ if $E_{BALL} > 0.75\, E_{CM}$.

2. Beam-gas and beam-wall interactions deposit a lot of energy at small angles; we therefore demand: $E_{TUNNEL}/E_{BALL} < 0.5$, where E_{TUNNEL} is the sum of the energies deposited in the 60 tunnel crystals of the main ball. This cut is almost 100% contained in the next cut. It is only noted for completeness.

3. Against beam wall and beam gas we cut in the following quantities: We define the absolut value of the vector sum $\beta = \frac{1}{E_{BALL}} \left| \sum_{i=1}^{672} E_i \hat{n}_i \right|$, where $\hat{n}_i$ is a unit vector pointing to the center of the i^{th} crystal, and the normalized transverse energy of an event $E_{trans} \quad \frac{1}{E_{CM}} \sum_{i=1}^{672} E_i \sin\theta_i$. We apply the following cut in the (β, E_{trans}) plane: events are accepted if they satisfy $E_{trans} > 0.2$, $\beta < 0.7$, and $E_{trans} > 0.5\beta + 0.1$. This cut is represented as a line in figure 4 where we show the (β, E_{trans}) plane for a representative subsample of all recorded ON $\Upsilon(4S)$ events and for events with separated beams, where we expect no multi - hadron events. Clearly visible is the rejection of the non e^+e^- events. This cut in E_{trans} requires implicitely a minimal energy $E_{BALL} > 0.2 E_{CM} \quad 2.1\ GeV$ at the $\Upsilon(4S)$ resonance.

An event which is accepted by all those cuts is called a hadronic event.

4.2 Electron Selection

A *bump* crystal is defined by a local maximum of energy deposited in a $CONREG$. Each *bump* together with its 12 closest neighbouring crystals form one cluster. The direction of the cluster (in φ and θ) is obtained by an energy weighted sum of the directions of the center of the 13 crystals. The energy assigned is the sum of

the energies of the 13 crystals with a small empirical correction, depending on a ratio of energies deposited in the 13 crystals. On an electron candidate we impose the following requirements:

- The pattern of the lateral energy distribution in the NaI must be consistent with that expected for a single electromagnetically showering particle.
- The angle between the cluster direction and the beam axis must give $|\cos\theta| < 0.70$ which is within the solid angle covered by all 4 tube chambers.
- At least 3 hits in the chambers must be consistent with the direction of the cluster.

Figure 5a shows the electron spectrum obtained after those cuts. In order to show the full spectrum the data is plotted using a logarithmic binning of 3% width. That kind of binning results in an approximately constant resolution per bin over the entire energy range. A clear signal around 1.5 GeV energy is visible in the ON $\Upsilon(4S)$ data but not in the continuum data. On the $\Upsilon(4S)$ there is still a large background from continuum events. Therefore in order to further more suppress non $B\bar{B}$ events, we demand the number of *bumps* to be > 7. Figure 6a shows the number of *bumps* for events which have an electron in the energy range $1.5\ GeV < E_e < 2.7\ GeV$. Compared are ON $\Upsilon(4S)$ data with the continuum data. In addition a Monte Carlo estimate of background from $\tau\bar{\tau}$ events is overlayed. In figure 6b the continuum subtracted distribution of ON $\Upsilon(4S)$ events is shown, together with a Monte Carlo prediction for $\Upsilon(4S) \rightarrow B\bar{B}$ events. Continuum and $\tau\bar{\tau}$ events have a low multiplicity. Further suppression of the non $B\bar{B}$ events is achieved by a cut in the Fox-Wolfram event shape parameter $H2$ [15]

$$H2 = \frac{\sum_{i,j} E_i E_j (3\cos^2\alpha_{i,j} - 1)}{2(\sum_i E_i)^2} < 0.55, \qquad (8)$$

where E_i is the energy deposited in the *bump* crystal i and α is the angle between *bumps*. Only *bumps* in the main ball excluding endcaps are used. The cut in the $H2$ parameter is illustrated in figure 7a and 7b. The last two cuts are placed in such a way that almost no $\Upsilon(4S)$ events are lost ($< 0.5\%$) which avoids an increase of the systematic uncertainties. But almost all remaining QED and $\tau\bar{\tau}$ events are rejected. The rejection of the remaining QED Bhabha events which radiated a photon or showered in the beam pipe is shown in figure 8. Bhabha events contain only electromagnetically showering particles and therefore deposit all their energy in the ball. After the cut on $H2$ and the number of *bumps* the

peak due to Bhabha events at E_{CM} is removed. Figure 5b shows that these two cuts reduce the continuum contribution to the electron spectrum above 1.5 GeV by more than a factor of 2. In the following only the spectrum above ≈ 1.5 GeV is analyzed since there the efficiency is under control and the background is small. We turn to a linear binning, when plotting the spectrum. This is reasonable, because the resolution is approximately constant over this range. It has also the advantage of easier comparison with measurements by other groups.

4.3 Efficiency Calculation

To estimate the detection efficiencies the standard Lund string fragmentation program version 6.2 [12] was used to simulate the decay of $\Upsilon(4S) \rightarrow B\overline{B}$. The generated events are passed through a complete detector simulation. This simulation includes the following steps:

1. Electromagnetically interacting particles are handled by the electromagnetic shower development program EGS [16].

2. The interaction of hadrons is simulated with the GHEISHA 6 program [17].

3. Extra energy deposited in the crystals by beam related background is taken into account by adding special background events to the Monte Carlo events. These background events are obtained by triggering on every $10^7 th$ beam crossing, with no other condition.

4. The events are then reconstructed using our standard software and subjected to the same cuts as the data.

The hadronic detection efficiency for $\Upsilon(4S) \rightarrow B\overline{B} \rightarrow hadrons$ is found to be:

$$\epsilon_H = (93 \pm 1)\%.$$

For decays, where one B meson decays semileptonically into $e\nu X$ and the energy of the electron is greater than 500 MeV, the hadronic detection efficiency is

$$\epsilon_{He} \quad (93 \pm 0.5)\%.$$

The product of the hadronic event seletion efficiency ϵ_{He} and the electron selelection efficiency ϵ_e is the total electron efficiency $\epsilon = \epsilon_{He} \times \epsilon_e$. We use 2 different methods to determine the efficiency.

1. First we generate $\Upsilon(4S) \rightarrow B\bar{B}$ Monte Carlo events where one B meson decays semileptonically and the other one according to the standard LUND string fragmentation program. The events are then analyzed as described above. The total efficiency ϵ to find electrons in these events is shown in figure 9 by open circles. We then fit a third order polynomial to the points the solid line. The dashed lines mark a $\pm 5\%$ deviation from the fit function.

2. Monte Carlo generated electrons are merged isotropically into selected high multiplicity "ON $\Upsilon(1S)$" hadronic events. We require, in addition to the hadron selection, that the hadronic event has more than 6 *bumps*. This is done in order to reduce the $\simeq 20\%$ contribution from $q\bar{q}$ and $\tau\bar{\tau}$ events to the ON $\Upsilon(1S)$ data sample. Merging electrons isotropically into low multiplicity (two jet like events) results in too high an efficiency, because the overlap of the merged electron with other particles becomes less likely. This method gives a measurement of ϵ_r and we assume $\epsilon = \epsilon_r \times 0.93$ for those events too. The solid points in figure 9 show the result obtained by this method.

We then compare the two resulting efficiencies in figure 9. At lower electron energies the merging method results in a significantly higher efficiency. This is due to the fact that in the merging method the electrons are distributed isotropically in the events. But for slow electrons from $B \rightarrow e\nu D, D^*$ decays the probability for the electron is high to overlap with the decay products of the D, D^* mesons, while at higher electron energies the electron is more likely backwards to the D or D^* meson. This was confirmed by the comparison of the efficiencies to detect electrons in $\Upsilon(4S)$ Monte Carlo events and to detect merged electrons in the same Monte Carlo events. We use the fitted line of figure 9 for the electron efficiency. From the comparison of the efficiencies obtained by the 2 methods we get a systematic error on the efficiency of $\Delta\epsilon/\epsilon \simeq 5\%$ for electron energies above 1.5 GeV, where the two efficiencies obtained by the different methods agree.

4.4 Background Estimation

Besides electrons from $b \rightarrow c$ and $b \rightarrow u$ transitions, those from $c \rightarrow s$ are present. In addition the following background sources contribute:

1. Charged hadrons and photons faking electrons.

   - The contribution from photons faking electrons is determined by measuring the neutral energy spectrum and scaling it down by the conversion probablity in the beam pipe and the chambers. The neutral

spectrum measured – continuum subtracted – is shown in figure 10a. This spectrum has still to be multiplied by the conversion probability ($p_{convert}$) to obtain the fake electron contribution from photons. This conversion probability varies from 4.6% at 1 GeV to 9% at 2 GeV. This change comes from the fact that most of the photons come from π^0 decays. At 2 GeV nearly all photons from a π^0 form a single cluster and the probability to find it charged is $1 - (1 - p_{convert})^2$. The conversion probability for a single photon is obtained by analyzing $e^+e^- \rightarrow \gamma\gamma$ events.

- We find the background from charged hadrons from B meson decays to the electron spectrum above 1.5 GeV to be less than 2 events. This number is deduces in two ways. First of all one has to take into account that the momentum spectrum of particles from B meson decays becomes zero for momenta larger than ≈ 2.7 GeV – see chapter 2. Hence the spectrum of particles is much softer than that obtained from decays of the $\Upsilon(1S)$ resonance or continuum events. The energy response of the Crystal Ball to hadrons is such that only a small fraction of the total energy is seen. Figure 11 shows the deposited energy of Monte Carlo generated π^+ of 2.0 and 2.5 GeV energy. Restricting the analyzed energy range to $E_e > 1.5$ GeV a reduction factor of 200 is achieved. Applying the pattern cuts for selecting electromagnetically showering particles the rejection factor is increased by a factor of 25. Assuming 0.1 charged hadrons with energy greater than 1.5 GeV per $B\bar{B}$ event we calculate a background of < 2 charged hadrons from 60000 $B\bar{B}$ events. In addition we measure the charged hadron background by the energy loss, dE/dx, in the wire chamber, which is different compared to that of electrons. Figure 12 shows the pulse height distributions of different particle types obtained by summing up the pulse heights from the individual layers, corrected for different pathlengths in the tube chambers. The background contribution is then obtained by comparing the electron spectra resulting from two different cuts in the chamber pulse height. The charged hadron background spectrum obtained in this way is displayed in figure 10. Also this method gives a background of 1 ± 1.0 events. A detailed discussion can be found in [2].

- The hadron and photon backgrounds together are less than 1 % of the $\Upsilon(4S)$ contribution for energies above 1.5 GeV . At about 1.5 GeV

the background from photons dominates, while towards lower energies the contribution from charged hadronic background becomes dominant. Below 1.5 GeV the background contribution from charged hadronic background through rises exponentially towards lower energies. This is the reason for the peak at $\approx 200\ MeV$ from minimum ionising charged hadrons in the observed electron spectrum (Figure 5b).

2. Contribution from the continuum productions. For this contribution we take a smooth function, which is obtained by a fit to the continuum data. Figure 14a shows the spectrum obtained from the continuum data sample together with the smooth function fitted to the data.

4.5 Method used to extract Branching Ratios and Kobayashi - Maskawa Matrix Elements from the Spectra

The predicted spectra are boosted with the B momentum to the $\Upsilon(4S)$ rest frame, folded with the energy resolution of the detector and corrected by our detection efficiency. The size of those two corrections is shown in figure 13. In detail the efficiency correction is done in the following way: let $d\Gamma/dE_e$ be the predicted electron spectrum from B meson decays boosted to the $\Upsilon(4S)$ center of mass system and folded with the energy resolution. Then T is the expected spectrum for a 100% braching ratio (e.g. for the channel $b \to c$),

$$T_{b\to c}(E_e) = \frac{d\Gamma_{cb}}{dE_e}\frac{1}{\Gamma_{cb}}\{\epsilon_e(E_e)\,\epsilon_{He}(E_e)\}\frac{2\,N_{BB}^{obs}}{\epsilon_H} \qquad (9)$$

with $N_{BB}^{obs} = N_H^{obs}(ON\ \Upsilon(4S)) - r \times N_H^{obs}(continuum)$

and Γ_{cb} the partial width of the models used.

I.e. using WSB's model one has to replace Γ_{cb} by $\Gamma(B \to c\nu D, D^*)$. $N_H^{obs}(ON\ \Upsilon(4S))$ and $N_H^{obs}(continuum)$ are the numbers of hadrons found on the $\Upsilon(4S)$ resonance and in the continuum respectively. $r = 4.028 \pm 0.009$ is the ratio of ON $\Upsilon(4S)$ and continuum luminosities corrected for the difference in beam energy. As noted in equation (9) the two hadron efficiencies ϵ_{He} and ϵ_H cancel each other. Therefore also systematic errors of the event simulation program cancel too.

We use the following functions to describe the measured electron spectra:
$Y_i = Y(E_e)$ is the functional form accounting for the observed electron spectrum from the $\Upsilon(4S)$ data

$$Y(E_e) = C \times T_{b\to c}(E_e) + \frac{U}{C} \times C \times T_{b\to u}(E_e)$$

$$+ \mathcal{S} \times T_{c\to}(E_c) + \mathcal{B} \times F(E_c) + \mathcal{K} \times Q(E_c) \qquad (10)$$

The quantities $\mathcal{C}, \frac{\mathcal{U}}{\mathcal{C}}, \mathcal{S}, \mathcal{B}$, and $\mathcal{K}$ are explained in detail now. After fitting with equation (10) to the data, the intensities $\mathcal{C}, \mathcal{S}$ are the measured branching ratios. Using e.g. the model of WSB yields $\mathcal{C} = BR(B \to c\nu D, D^*)$.
$\frac{\mathcal{U}}{\mathcal{C}}$ is the ratio of branching ratios. For WSB's model we get $\frac{\mathcal{U}}{\mathcal{C}} \equiv \frac{BR(B\to c\nu\pi,\rho)}{BR(B\to c\nu D,D^*)}$.
The Kobayashi - Maskawa matrix elements are obtained by, see equation 2 and table 1

$$|V_{cb}|^2 \equiv \mathcal{C}/(\tau_B \times \hat{\Gamma}_{cb})$$

with τ_B being the B meson lifetime. In the model of WSB the part of the electron spectrum used in the fit corresponds to transitions $B \to c\nu D, D^*$ only, hence $\hat{\Gamma}_{cb} \equiv \hat{\Gamma}(B \to c\nu D, D^*)$ The ratio of matrix elements is obtained by:

$$|V_{ub}/V_{cb}|^2 = \frac{\mathcal{U}}{\mathcal{C}} \times \hat{\Gamma}_{cb}/\hat{\Gamma}_{ub}$$

e.g. using the model of WSB's one has to replace $\hat{\Gamma}_{cb} \equiv \hat{\Gamma}(B \to c\nu D, D^*)$ and $\hat{\Gamma}_{ub} \equiv \hat{\Gamma}(B \to c\nu\pi, \rho)$. Analoguos considerations hold for GIW's model.

Q is the continuum contribution described by a smooth function
$Q(E_c) = \exp(\alpha E_c^1 + \beta E_c^2 + \gamma E_c^3 + \delta E_c^4)$ with $\alpha, \beta, \gamma, \delta$ free parameters determined by the fit. F represents the fake electrons. $V_i = V(E_c)$ is the functional form accounting for the observed electron spectrum from the continuum data

$$V(E_c) = \mathcal{K}_C \cdot Q(\alpha, \beta, \gamma, \delta) \qquad (11)$$

We perform a maximum likelihood fit with Poissonian error distribution. The fit is done simultaneously to the binned $\Upsilon(4S)$ data $N^{obs}(E_c) \equiv N_i$, and to the binned continuum data $M^{obs}(E_c) \equiv M_j$. The likelihood function is defined by:

$$\mathcal{L} = \prod_i \left(\frac{e^{-V_i} \cdot V_i^{N_i}}{N_i!}\right) \times \prod_j \left(\frac{e^{-V_j} \cdot V_j^{M_j}}{M_j!}\right)$$
$$\times \exp\left(-\frac{(\mathcal{B} - \mathcal{B}_m)^2}{2\sigma_{\mathcal{B}}^2}\right) \times \exp\left(\frac{(\mathcal{K} - r \cdot \mathcal{K}_C)^2}{2\sigma_{\mathcal{K}}^2}\right) \qquad (12)$$

Here the first and second term represent the likelihoods for the $\Upsilon(4S)$ and continuum data. The 3^{rd} and 4^{th} term form constraints. The first one constrains the background intensity $\mathcal{B}$ by the measured background intensity $\mathcal{B}_m$, the second restricts the intensity of the continuum contribution $\mathcal{K}$ to the measured product of continuum intensity $\mathcal{K}_C$ times the luminosity ratio r. To compare results from different fits we calculate a χ^2 according to [19] from the result of the fit:

$$\chi^2 = 2\sum_i (V_i - N_i + N_i \ln\frac{N_i}{V_i}) \qquad (13)$$

The intensities $C, \mathcal{B}, \frac{u}{c}, \mathcal{S}, \mathcal{K}, \mathcal{K}_C$ and continuum parameters $\alpha, \beta, \gamma, \delta$ are determined by the fit. As the background ($\mathcal{B}$) and the $c \rightarrow s$ ($\mathcal{S}$) contributions above $E_e \approx 1.5\ GeV$ are small and rather similar in shape, the intensity $\mathcal{B}$ is very correlated to the $c \rightarrow s$ intensity $\mathcal{S}$. Due to the constraint in the likelihood for $\mathcal{B}$ with $\sigma_{\mathcal{B}}/\mathcal{B} = 1$ the fitted $\mathcal{B}$ is in partice not a free parameter, but comes out to be exactly at the measured $\mathcal{B}_M$ value. The parameters $\alpha, \beta, \gamma, \delta$ are determined by both, the $\Upsilon(4S)$ data and the continuum data. This method is useful, as we have only a small continuum data sample. The continuum contribution in the $\Upsilon(4S)$ fit is constrained in shape and intensity by the data between $E_e = 2.6\ GeV$ and $4\ GeV$ where we assume no other contributions. This method gives confidence in the function representing the continuum contribution. The result agrees well with the predicted shape from the fit to the continuum data alone. For the intensity of the continuum contribution we find that the fitted value $\mathcal{K}$ is within 0.08% of the value $r \times \mathcal{K}_C$ expected from the luminosity ratio, with $\sigma_{\mathcal{K}}/\mathcal{K} = 1\%$ used in the constraint (12). A fit with the continuum function Q to the continuum data alone gives a $\chi^2/d.o.f. = 60.6/63 \approx 56\%$ C.L. Other functions like a polynomial and / or single exponentials give a χ^2 much worser. All contributions to the ON $\Upsilon(4S)$ spectrum are shown in figure 14b. The background from charged hadrons and photons faking electrons is added up and displayed as a single line. The efficiency corrected, continuum and background subtracted spectrum normalized to the number of produced B mesons, is shown in figure 15 and listed in appendix A. As we want to measure $b \rightarrow c$ and $b \rightarrow u$ contributions only, we use the data above $E_e = 1.5\ GeV$, where the $c \rightarrow s$ *and* fake electron contributions are small. Using the data below $E_e = 1.5\ GeV$ would require a very accurate knowledge of the background and the $c \rightarrow s$ intensities and shapes.

5. Results on the Ratio of Branching Ratios $(b \rightarrow u)/(b \rightarrow c)$ and on $|V_{ub}/V_{cb}|$

Here and in the following chapter we present and discuss the results of the fit of the data, as shown in figure 14, to formula 10 which contains the electron spectrum shape and the branching ratios of its various contributions. The MINUIT [18] program has been used. For the $b \rightarrow c$ and $b \rightarrow u$ spectrum shapes the theoretical models described in chapter 2 are used.

The first glance shows that the measured electron spectrum from B meson decays does not extend to $E_e > 2.4\ GeV$ no $b \rightarrow u$ transition is seen and we will give upper limits.

Starting with ACM's model, we cannot determine from our measured spectrum the free parameter m_u with meaningful errors, because no significant $b \to u$ signal is found. We therefore calculate the upper limit for various values for the u quark mass m_u shown in figure 16. For higher masses the upper limit gets weaker, because the predicted spectrum becomes softer and comparable to the spectrum from $b \to c$ decays. A u quark mass $m_u = m_c$ would result in no upper limit as then the $b \to c$ and $b \to u$ predictions are identical. For u quark masses below 400 MeV/c^2 the upper limit is independent of m_u. Henceforth we use $m_u = 150 MeV/c^2$ as in the paper by ACM.

The upper limit obtained with the different models are shown in figures 17 and 18 as a function of the lower fit range in the electron spectrum.

Using ACM's model with p_F and m_c free we obtain an upper limit

$$BR(B \to e\nu X_u)/BR(B \to e\nu X_c) < 4.5\% \text{ and } |V_{ub}/V_{cb}| < 0.15 \text{ at } 90\% \text{ C.L.}$$

The best fit values for those parameters are: $p_F = (388 \pm 52)\ MeV/c$ and $m_c = (1607 + 46)\ MeV/c^2$. With equation (6) we obtain for the b quark mass an average value $< m_b > = (4.85 \pm 0.68) GeV/c^2$ where $|\vec{P}| = p_F$ was used.

In order to get the $(b \to u)/(b \to c)$ values independent of the measured $b \to c$ contribution we increase the lower fit limit to higher energies, where the $b \to c$ contribution becomes smaller and goes to zero above $E_e = 2.4\ GeV$. Fixing all the parameters to the best values previously found – also the $b \to c$ contribution C but not the $(b \to u)/(b \to c)$ intensity $\frac{u}{c}$) – we obtain an upper limit

$$BR(b \to e\nu u)/BR(b \to e\nu c) < 5.4\% \text{ or } |V_{ub}/V_{cb}| < 0.16 \text{ at } 90\% \text{ C.L.}$$

independent of the $b \to c$ contribution in this energy range (see figures 17 and 18).

As the GIW model has no precise prediction for $b \to u$ with $E_e < 2.2\ GeV$, we proceed in the following way: we determine the intensity C of the $b \to c$ transition for electron energies $E_e > 1.5\ GeV$ together with a free $b \to u$ intensity $\frac{u}{c}$, then fix the $b \to c$ intensity C, background B and continuum contribution K and finally find the upper limit on

$$\frac{BR(B \to e\nu X(1S, 1P, 2S)_u)}{BR(B \to e\nu X(1S, 1P, 2S)_c)} < 4.6\% \text{ or } \left|\frac{V_{ub}}{V_{cb}}\right| < 0.216 \text{ at } 90\ \% \text{ C.L.}$$

for the spectrum above $E_e > 2.2\ GeV$ (see figures 17 and 18).
For electron energies $E_e > 2.4\ GeV$, where the $b \to c$ contribution is zero – but using the previously measured $b \to c$ contribution – we find

$$\frac{BR(B \to e\nu X(1S, 1P, 2S)_u)}{BR(B \to e\nu X(1S, 1P, 2S)_c)} < 6.5\% \text{ or } \left|\frac{V_{ub}}{V_{cb}}\right| < 0.26 \text{ at } 90\ \% \text{ C.L.}$$

Employing the WSB model results in an upper limit on

$$\frac{BR(B \to e\nu\pi,\rho)}{BR(B \to e\nu D, D^*)} < 2.5\% \text{ or } |\frac{V_{ub}}{V_{cb}}| < 0.15 \text{ at 90 \% C.L.}$$

using the data above $E_e = 2.3$ or $2.4\ GeV$. For the KS model we obtain an upper limit on

$$\frac{BR(B \to e\nu\pi,\rho)}{BR(B \to e\nu D, D^*)} < 3.0\% \text{ or } |\frac{V_{ub}}{V_{cb}}| < 0.14 \text{ at 90 \% C.L.}$$

when using the data above $E_e = 2.3$ or $2.4\ GeV$.

6. Results on the Branching Ratio $B \to e\nu X_c$ and on $|V_{cb}|$

Model	$BR(B \to e\nu X_c)$ [%]	$\|V_{cb}\|$ 10^{-2}	$(b\to u)/(b\to c)$ 10^{-2}	χ^2 d.o.f.
ACM p_F and m_c free, best $p_F = (388 \pm 52)\ MeV/c$ $m_c = (1607 \pm 46)\ MeV/c^2$	$12.0 \pm 0.5 \pm 0.7$	5.3 ± 0.5	1.6 ± 1.6	39.2/40
GIW ; X=(1S,1P,2S)	$11.9 \pm 0.4 \pm 0.7$	4.2 ± 0.5	2.0 ± 1.3	39.9/42
GIW + AW	$11.9 \pm 0.4 \pm 0.7$	5.1 ± 0.5		
WSB ; X = (1S)	$10.8 \pm 0.4 \pm 0.7$	5.5 ± 0.5	$0.0\ ^{+0.8}_{-0.0}$	39.8/38
KS ; X (1S)	$10.1 \pm 0.5 \pm 0.7$	5.0 ± 0.5	$0.6\ ^{+1.7}_{-0.6}$	40.2/38
PS ; X (1S)	$14.1 \pm 0.8 \pm 0.7$	4.0 ± 0.6		35.5/38
Average; X all **ACM+AW+WSB+KS**	$11.7 \pm 0.5 \pm 0.7$	5.2 ± 0.5		

Table 3: Results on $BR(B \to e\nu X_c)$ and $|V_{cb}|$ The errors quoted are: statistical and systematic for the branching ratio measurement and experimental in the case of $|V_{cb}|$. The experimental error of V_{cb} is calculated by adding the statistical and systematic error and that of the the B meson lifetime in quadrature. It is dominated by the B meson lifetime measurement. The error on $|V_{cb}|$ due to theoretical uncertainties quoted by all theories is about 10%.

If the $b \to u$ contribution would not be small, it would be incorrect to measure the inclusive $b \to c$ intensity with the models by GIW, WSB, KS and PS which do not fully predict the $b \to u$ spectrum at lower electron energies where the $b \to c$

intensity is determined. However, since the $b \to u$ contribution is small and we can calculate the branching ratio $BR(B \to e\nu X_c)$ and $|V_{cb}|$ using all meson decay models. With free $b \to u$ contributions, which are not significant and therefore only quoted for completeness, and a B meson lifetime of $\tau_B = (1.13 \pm 0.14) \times 10^{-12} sec$ [20] we get the results listed in table 3. The models of ACM, GIW with the AW correction, WSB, and KS give consitent results. The model by PS gives a very high branching ratio of 14.1% for the 1S states alone. This is due to the fact, that the predicted spectrum is very soft and only the high energy part is fitted. The model can not describe the lower energy part, where the predicted spectrum lies above the measured one, when fixing the amplitude by the fit to energies greater than 1.7 GeV, where only D and D^* contribute. This model can therefore be ruled out by our measurement and is not used any further. If we assume that the higher spin states which have not been calculated - add 10% to WSB'sand KS's branching ratio we get an average total branching ratio: $BR(B \to e\nu X_c) = (11.7 \pm 0.4 \pm 0.7)\%$ for all four models. Applying the correction by AW to GIW's we average the results from the four models and obtain $|V_{cb}| = 0.052 \pm 0.005 \pm 0.005$.

7. Systematic Errors

For the $(b \to u)/(b \to c)$ limit the knowledge of the absolute energy scale is essential. The scale of the measured energy has been found to be
$E_{true} = E_{measured}(-5 \pm 6) MeV$ at 2 GeV. The energy measurement is done in the following way:

- The crystals are calibrated at beam energy ($\approx$ 5 GeV) with Bhabha events and scaled linearly.
- An empirical correction for lower energies up to 600 MeV has been tested [21] with 2 photon reactions forming π^0, η, η' in the processes $e^+e^- \to e^+e^-\pi^0, \eta, \eta' (\to \gamma\gamma)$ and with photons from the processes $\Upsilon(2S) \to \gamma\gamma\Upsilon(1S) \to \gamma\gamma l^+l^-$ and $\Upsilon(2S) \to \pi^0\pi^0\Upsilon(1S) \to \pi^0\pi^0 l^+l^-$, $l^{+/-}$ standing for electrons or muons. Another test energy at 600 MeV below E_{BEAM} at has been obtained by analyzing Bhabha events from the $\Upsilon(1S)$ resonance with the energy scale obtained by the $\Upsilon(4S)$ data/ Both datasamples were taken within two days. This empirical correction predicts that the energy measurement is (25 ± 4) MeV too low for an electron of 2 GeV.
- This effect is more than compensated by:

- Extra energy of $(+23 \pm 5)$ MeV added to the electron energy from other particles in the hadronic event. This was tested by comparing the energy measured for Monte Carlo electrons in the "empty" ball and in hadronic events.
- A $(+7 \pm 1)$ MeV correction at 2 GeV to the measured energy due to the electron selection used in this analysis, which prefers to select more electrons with a higher energy response in the crystals than the cuts used in the calibration procedure.

The contributions to the systematic error of the $b \to c$ measurement are:

- Varying the energy scale within the limits obtained above gives no visible effect for the $b \to c$ branching ratio.
- The largest contribution to the systematic error on the $b \to c$ branching ratio is $\Delta BR/BR \simeq 6\%$. It comes from the efficiency determination, to which we assigned an error of $\Delta\epsilon/\epsilon \simeq 5\%$.

Other sources of systematic errors are:

- relative efficiency to accept an event as hadronic for events where one B meson decays semileptonically compared to all other decays $\Delta\epsilon/\epsilon \simeq 1\%$,
- number of observed $\Upsilon(4S)$ events $\Delta N/N \simeq 2\%$,
- varying the fit range gives a change of less than 1% in $\Delta BR/BR$,
- changing the energy scale by 10 MeV changes $\Delta BR/BR$ by less than 1%.

The total systematic error is obtained by adding the individual sources in quadrature. For the measurement of the ratio $(b \to u)/(b \to c)$ we have verified that

- the efficiency for the $b \to u$ channel is the greater or equal compared to that for the $b \to c$ channel.
- the upper limit becomes smaller, if one scales the measured electron energy to lower energies.

8. Comparison with other Experiments

8.1 Comparison with results from ARGUS [22] [23] [24]

ARGUS quotes an upper limit on $\frac{BR(B \to e\nu X(1S,1P,2S)_u)}{BR(B \to e\nu X(1S,1P,2S)_c)} < 6\%$ obtained with GIW's model in the electron energy range $E_e > 1.6\ GeV$. With a modified free quark spectator model and a limited data sample of 12 pb^{-1} ARGUS gets a branching ratio $BR(B \to e\nu X_c) = (12.0 \pm 0.9 \pm 0.8)\%$. ARGUS has measured the decays $B^+ \to p\bar{p}\pi^+$ and $B^0 \to p\bar{p}\pi^+\pi^-$ with branching ratios of $(3.7 \pm 1.3 \pm 1.4)\ 10^{-4}$ and $(6.0 \pm 2.0 \pm 2.2)\ 10^{-4}$, respectively. From these measurements they deduce a lower limt of $|V_{ub}/V_{cb}| > 0.07$.

8.2 Comparison with results from CLEO [1] [25]

Beside other models CLEO used ACM's model with a parameter choice fixed to $p_F = 215\ MeV/c$ and $m_c = 1700\ MeV/c^2$. They get an upper limit of

$$\frac{BR(B \to e\nu X_u)}{BR(B \to e\nu X_c)} < 2.7\% \text{ at } 90\ \% \text{ C.L.}$$

A branching ratio $BR(B \to e\nu X_c) = (11.0 \pm 0.3 \pm 0.7)\%$ is measured. Using the same fit parameters the Crystal Ball experiment obtains

$$\frac{BR(B \to e\nu X_u)}{BR(B \to e\nu X_c)} < 2.6\% \text{ at } 90\ \% \text{ C.L.}$$

and $BR(B \to e\nu X_c) = (11.0 \pm 0.4 \pm 0.7)\%$ with a $\chi^2/d.o.f. = 43/42$ - a very similar result.

8.3 Comparison with results from CUSB [26]

Using ACM's model with a fixed parameter setting of $p_F = 150\ MeV/c$ and $m_c = 1700\ MeV/c^2$ an upper limit of

$$\frac{BR(B \to e\nu X_u)}{BR(B \to e\nu X_c)} < 5.5\% \text{ at } 90\ \% \text{ C.L.}$$

is obtained. A branching ratio $BR(B \to e\nu X_c) = (9.0 \pm 3.0)\%$ is measured. Doing the same we obtain

$$\frac{BR(B \to e\nu X_u)}{BR(B \to e\nu X_c)} < 1.5\% \text{ at } 90\ \% \text{ C.L.}$$

and $BR(B \to e\nu X_c) = (10.7 \pm 0.4 \pm 0.7)\%$ with a $\chi^2/d.o.f. = 52/42$.

9. Conclusions

With the Crystal Ball detector we have measured the inclusive electron spectrum from $\Upsilon(4S)$ decays. Using four different theoretical models for the matrix elements and the shape of the electron spectrum an average branching ratio

$$BR(B \to e\nu X_c) = (11.7 \pm 0.4 \pm 0.7)\%$$

has been obtained. The model by PS can be ruled out, it does not fit to the data. The average result on the Kobayashi - Maskawa matrix element is

$$|V_{cb}| = 0.052 \pm 0.005 \perp 0.005$$

using four models - with the correction by AW to GIW's model. For the ratio of $|V_{ub}/V_{cb}|$ we obtain an upper limit dependent on the model used. WSB,KS and ACM give a conservative upper limit of

$$|V_{ub}/V_{cb}| < 0.15 \text{ at } 90\%\text{C.L.},$$

if one uses the data above $E_e = 2.4\ GeV$ where no $b \to c$ contribution is present. GIW gives a significantly weaker upper limit of

$$|V_{ub}/V_{cb}| < 0.26 \text{ at } 90\%\text{C.L.},$$

due to the softer spectrum in the $b \to u$ channel and due to the larger semileptonic width predicted for the $b \to c$ channel. Applying the AW correction to the $B \to e\nu D^*$ channel the upper limit goes down to $|V_{ub}/V_{cb}| < 0.21$.

10. Acknowledgement

We would like to thank the DESY and SLAC directorates for their support. This experiment would not have been possible without the dedication of the DORIS machine group as well as the experimental support groups at DESY. Those of us from abroad wish to thank the DESY laboratory for the hospitality extended to us while working at DESY. We acknowledge useful discussions with M. Bauer,J.G. Körner, R. Rückl,G.A. Schuler, B.Stech and M. Wirbel. Z.J., B.M., and G.N. thank DESY for financial support. D.W. acknowledges support from the National Science Foundation. E.D.B., R.H., and K.S. have benefitted from financial support from the Humboldt Foundation. S.C. acknowledges support from the Dept. of Physics and Laboratory of Nuclear Science of the Massachusetts Institute of Technology. The Nijmegen group acknowledges the support of FOM-ZWO. The Erlangen, Hamburg, and Würzburg groups acknowledge financial support from the German Federal Minister for Research and Technology (BMFT) under the

contract numbers 054 ER 11P(5), 054 HH 11P(7), 054 WU 11P(1) and from the Deutsche Forschungsgemeinschaft (Hamburg). This work was supported in part by the U.S. Department of Energy under Contract No. DE-AC03-81ER40050 (CIT), No. DE-AC02-76ER03064 (Harvard), No. DE-AC02-76ER03072 (Princeton), No. DE-AC03-76SF00515 (SLAC), No. DE-AC03-76SF00326 (Stanford), and by the National Science Foundation under Grants No. PHY75-22980 (CIT), No. PHY81-07396 (HEPL), No. PHY82-08761 (Princeton).

References

[1] M. Gilchriese, in: Proc. of the 23rd Int. Conf. on High Energy Physics, Berkeley, 1986; R. Poling, ibid.

[2] K. Wachs, Ph.D thesis, University of Hamburg, unpublished, 1988.

[3] M. Kobayashi and T. Maskawa, Prog. Theor. Phys. **49** (1973) 652.

[4] G. Altarelli, N.Cabibbo, G.Corbo, L.Maiani, G. Martinelli, Nucl. Phys. **B208** (1982) 365. In this paper refered to as ACM.

[5] B. Grinstein, M. B. Wise, N. Isgur, Phys. Rev. Lett. **56** (1986) 298 and California Institute of Technology preprint CALT-68-1311. In this paper refered to as GIW.

[6] M. Wirbel , B. Stech and M. Bauer, Z. Phys. **C29** (1985) 637. In this paper refered to as WSB.

[7] J.G. Körner and G.A. Schuler DESY 87-135 or MZ-TH/87-16. In this paper refered to as KS.

[8] J.G. H. Pietschmann and F. Schoeberl Europhys. Lett. **B** (1986) 583. In this paper refered to as KS.

[9] New measurements of the $\Upsilon(4S)$ and the B masses are reported in: D. Kreinick, Recent B Meson Results from CLEO, in: Proc. of The International Symposium on Production and Decay of Heavy Hadrons, Heidelberg, May,1986, K.R. Schubert, R. Waldi (Ed.);
S. Weseler, Experimental Review on B Meson Decays, in: Proc. of The International Symposium on Production and Decay of Heavy Hadrons, Heidelberg, May,1986, K.R. Schubert, R. Waldi (Ed.);
C. Bebec, Exclusive Decays and Masses of the B Mesons, The CLEO Collaboration, Cornell preprint CLNS, 86/742.

[10] N. Cabibbo and L. Maiani, Phys. Lett. **79B** (1978) 109.

[11] T. Altomari and L. Wolfenstein, Carnegie Mellon University preprint, CMU - HEP 86 - 1987. Refered to as AW in this paper.

[12] T. Sjøstrand, Lund preprint, LU TP 85-10, October 1985.
also CERN Pool programs W5035/W5045/W5046/W5047 long writeup.

[13] M. Oreglia *et al.*, Phys. Rev. **D25** (1985) 2259;
E. D. Bloom and C. W. Peck, Ann. Rev. Nucl. Part. Sci. **33** (1983) 143.

[14] D. Antreasyan *et al.*, DESY 87-054 and SLAC-PUB-4305, 1987

[15] G. C. Fox and S. Wolfram, Nucl. Phys. **B149** (1979) 413.

[16] R. Ford and W. Nelson, SLAC-210 (1978).

[17] H. Fesefeldt, Aachen preprint, PITHA 85/02

[18] Minimizer program from the CERN Pool programs long writeup D506.

[19] S. Baker and R.D. Cousins N.I.M. **221** (1984) 437.

[20] For a compilation of the B meson lifetime measurements see e.g. Sau Lan Wu, Lifetimes of Heavy Flavour Particles, talk given the International Symposium on LEPTON PHOTON Interactions at High Energies, Hamburg, July 27-31,1987.

[21] D. Gelphman *et al.*, Phys. Rev. **D32** (1985) 2893 and
D. Williams, Ph.D thesis (1987), Harvard University, unpublished

[22] K.R. Schubert, in: Proc. of the 23rd Int. Conf. on High Energy Physics, Berkeley, 1986.

[23] S. Weseler, Ph.D. thesis University of Heidelberg, unpublished, 1987.

[24] W. Schmitt - Parzefall, Talk given at the International Symposium on LEPTON PHOTON Interactions at High Energies, Hamburg, July 27-31,1987.

[25] T. Jensen, San Miniato 1987 2nd Topical Seminar on HEAVY FLAVOURS , San Miniato, May 25-29, 1987

[26] C. Klopfenstein *et al.*, Phys. Lett. **130B** (1983) 444.

Appendix A

The electron spectrum of B meson decays, normalized to the number of B mesons. Background and continuum contribution are subtracted. Data are corrected for detection efficiency. The errors quoted are statistical only. A common systematical error of $\Delta N/N = 6\%$ has to be added.

Energy $[GeV]$	$dN/(dEN_B)$ $[1/GeV\ 10^{-1}]$	error $[1/GeV\ 10^{-1}]$	Energy $[GeV]$	$dN/(dEN_B)$ $[1/GeV\ 10^{-1}]$	error $[1/GeV\ 10^{-1}]$
0.625	1.44	0.31	1.825	0.779	0.080
0.675	1.21	0.27	1.875	0.718	0.076
0.725	1.13	0.24	1.925	0.582	0.070
0.775	1.43	0.22	1.975	0.569	0.068
0.825	1.44	0.20	2.025	0.426	0.061
0.875	1.01	0.18	2.075	0.386	0.058
0.925	1.14	0.16	2.125	0.224	0.049
0.975	1.15	0.15	2.175	0.183	0.045
1.025	0.989	0.14	2.225	0.051	0.035
1.075	1.06	0.13	2.275	0.076	0.037
1.125	0.803	0.12	2.325	0.046	0.033
1.175	0.902	0.11	2.375	0.058	0.034
1.225	0.761	0.10	2.425	- 0.010	0.027
1.275	0.907	0.10	2.475	- 0.035	0.023
1.325	1.00	0.10	2.525	0.006	0.027
1.375	0.882	0.10	2.575	- 0.014	0.025
1.425	1.06	0.10	2.625	0.014	0.027
1.475	1.11	0.10	2.675	0.024	0.028
1.525	1.08	0.099	2.725	0.003	0.025
1.575	0.970	0.094	2.775	0.007	0.025
1.625	1.08	0.096	2.825	0.010	0.025
1.675	0.843	0.086	2.875	0.026	0.027
1.725	1.00	0.090	2.925	0.00	0.022
1.775	1.05	0.091	2.975	- 0.002	0.020

Figure Caption

1 $\sigma_{visible}$ as a function of center - of - mass energy in the $\Upsilon(4S)$ region. The curves are plotted to guide the eye.

2 The electron spectrum as predicted by ACM, GIW, KS, PS, and WSB, smeared with the detector resolution. The various predictions oare labelled with the authors symbols. Those parts where the predictions are complete are shown in bold symbols
a) The normalized spectrum, $\frac{N}{\Gamma}\frac{d\Gamma}{dE_e}$. $N = 1.0, 1.0, 0.9, 0.9, 0.9$ for the models ACM, GIW, WSB, KS, PS, respectively. In addition the prediction from the Lund Monte Carlo program for $c \rightarrow s$ is shown as a histogram.
b) $|V_{cb}|^2 d\Gamma_{cb}/dE_e$ and $|V_{ub}|^2 d\Gamma_{ub}/dE_e$

3 The Crystal Ball detector

4 Hadronic event sample: The β, E_{trans} plane. The events accepted are in the upper left part. No other cuts are applied.
a) Representative ON $\Upsilon(4S)$ data sample.
b) Separated beam data

5 The raw electron spectrum. Crosses: ON $\Upsilon(4S)$ data; circles: continuum data.
a) after electron selection cuts.
b) after additional cuts: number of *bumps* > 7, $H2 < 0.55$.

6 Number of *bumps* (multiplicity) for events with electron candidates with $1.5 < E_e < 2.7\ GeV$.
a) dots with error bars: ON $\Upsilon(4S)$ data; histogram: continuum data; shaded histogram: Monte Carlo $\tau\tau$ events.
b) dots with error bars: ON $\Upsilon(4S)$ data, continuum subtracted; histogram: $\Upsilon(4S) \rightarrow B\bar{B}$ Monte Carlo events.

7 H2 for events satisfying electron candidates with $1.5\ GeV < E_e < 2.7\ GeV$ and number of *bumps* > 7.
a) dots with error bars: ON $\Upsilon(4S)$ data; histogram: continuum data; shaded histogram: Monte Carlo $\tau\tau$ events.
b) dots with crosses: ON $\Upsilon(4S)$ data, continuum subtracted; histogram: $\Upsilon(4S) \rightarrow B\bar{B}$ Monte Carlo events.

8 E_{BALL} for ON $\Upsilon(4S)$ events with at least 1 electron candidate.
Histogram: without cut in number of *bumps* and $H2$. Shaded histogram: with cut in number of *bumps* > 7 and $H2 < 0.055$

9 Total electron detection efficiency. $\epsilon = \epsilon_{geo}\,\epsilon_e$
Open circles: from $\Upsilon(4S)$ Monte Carlo. Solid line: fit to open circles. Dashed line: fit $\pm 5\%$. Solid points: Efficiency from merging electrons into $\Upsilon(1S)$ data

10 Background contributions to the electron spectrum.
a) Neutral spectrum from $B\bar{B}$ decays measured with the same cuts employed for the electron spectrum. The continuum contribution has been subtracted from the ON $\Upsilon(4S)$ data by a smooth function fitted to the continuum data. The fit shown is used to describe the neutral spectrum from $\Upsilon(4S)$ decays. These data have still to be multiplied by the photon conversion efficiency.

b) Background from charged hadrons from $B\overline{B}$ decays to the observed electron spectrum. The shown fit is used to describe the charged background from $\Upsilon(4S)$ decays to the electron spectrum.

11 Energy deposited in the Crystal Ball by π^+ of 2.0 and 2.5 GeV energy, a Monte Carlo simulation. The peak at 0.2 GeV results from minimum ionizing particles.

12 The sum of the pulse heights (ph) from single particles in the proportional aluminum tube chambers for different particle types.
Solid line: 5 GeV electrons; solid histogram: 5 GeV muons; dashed histogram: low energy muons(of $\approx$ 100 MeV kinetic energy); crosses: minimum ionizing particles in hadronic events, selected by pattern cuts in the ball. The pulse height in each layer is normalized to the pulse height obtained with Bhabha events. The pulse height is corrected for the different pathlengths through the chamber due to different incident directions θ.

13 The electron spectrum as predicted by KS from $B \rightarrow e\nu\pi$ in the B meson rest frame, after boost to the $\Upsilon(4S)$ restframe $-\beta = 0.06$, and after smearing with the detector resolution.

14a The measured electron energy spectra. a) for continuum events. The fit shown is described in the text. Note the different bin size compared to that of the ON $\Upsilon(4S)$ data -figure 14b. The luminosity scale factor $r = 4.028$ practically compensates the factor 4 from the different bin size therefore the two plots can be directly compared. bin sizes. Therefore the 2 plots can directely be compared.

14b b) On the $\Upsilon(4S)$ resonance. The predictions shown are from ACM, they are corrected for detector response.

15 The inclusive electron energy spectrum from B mesons from $\Upsilon(4S)$ decays, corrected for efficiency and background subtracted. The data are normalized either to the number of produced B mesons (left hand scale) or to the integrated luminosity (right hand scale). Predictions are from the ACM model.

16 Upper limit on $BR(B \rightarrow e\nu X_u)/BR(B \rightarrow e\nu X_c)$ using ACM's model for different u quark masses. The curve is a smooth function fitted to the points to guide the eye.

17 Upper limit on $BR(B \rightarrow e\nu X_u)/BR(B \rightarrow e\nu X_c)$ for different models as funtion of the lower limit in the electron energy E_e used for the fit. Open symbols are for comparison only, as they are outside the valid fit ranges. For GIW and WSB only some final states have been calculated and therefore $X = (1S, 1P, 2S)$ for GIW and $X = 1S$ for KS and WSB.

18 Upper limit on $|V_{ub}/V_{cb}|$ for different models and fit ranges. Open symbols are for comparison only, as they are outside the valid fit ranges.

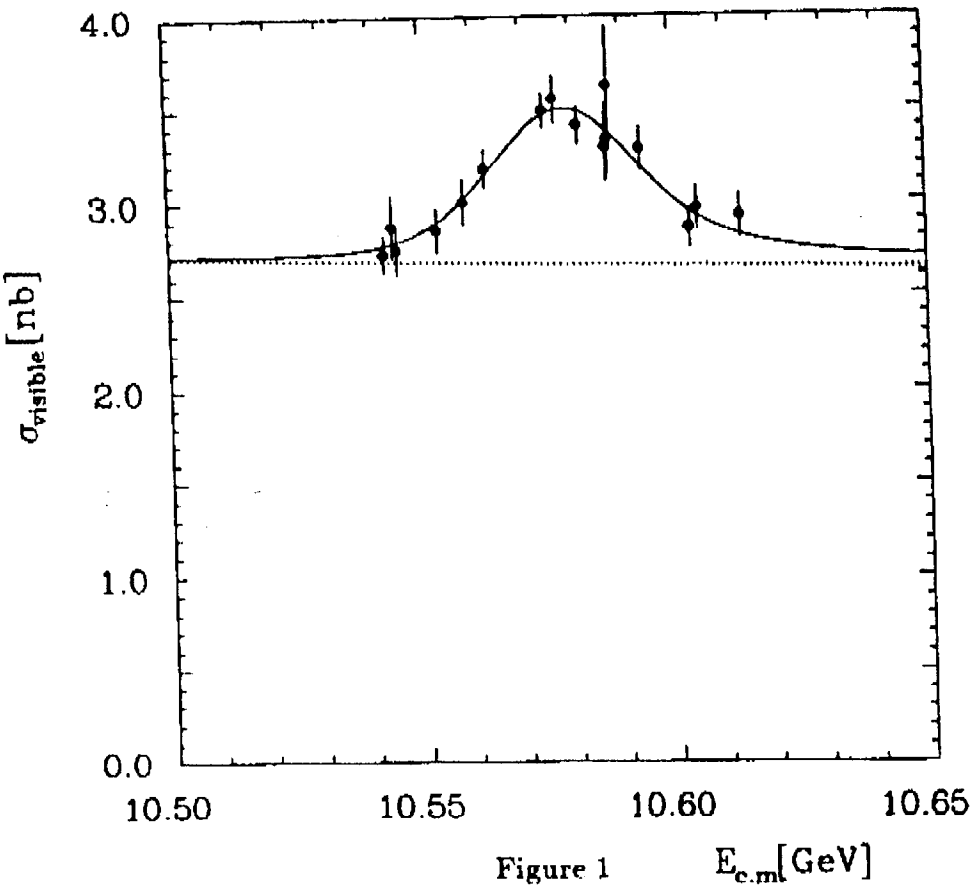

Figure 1

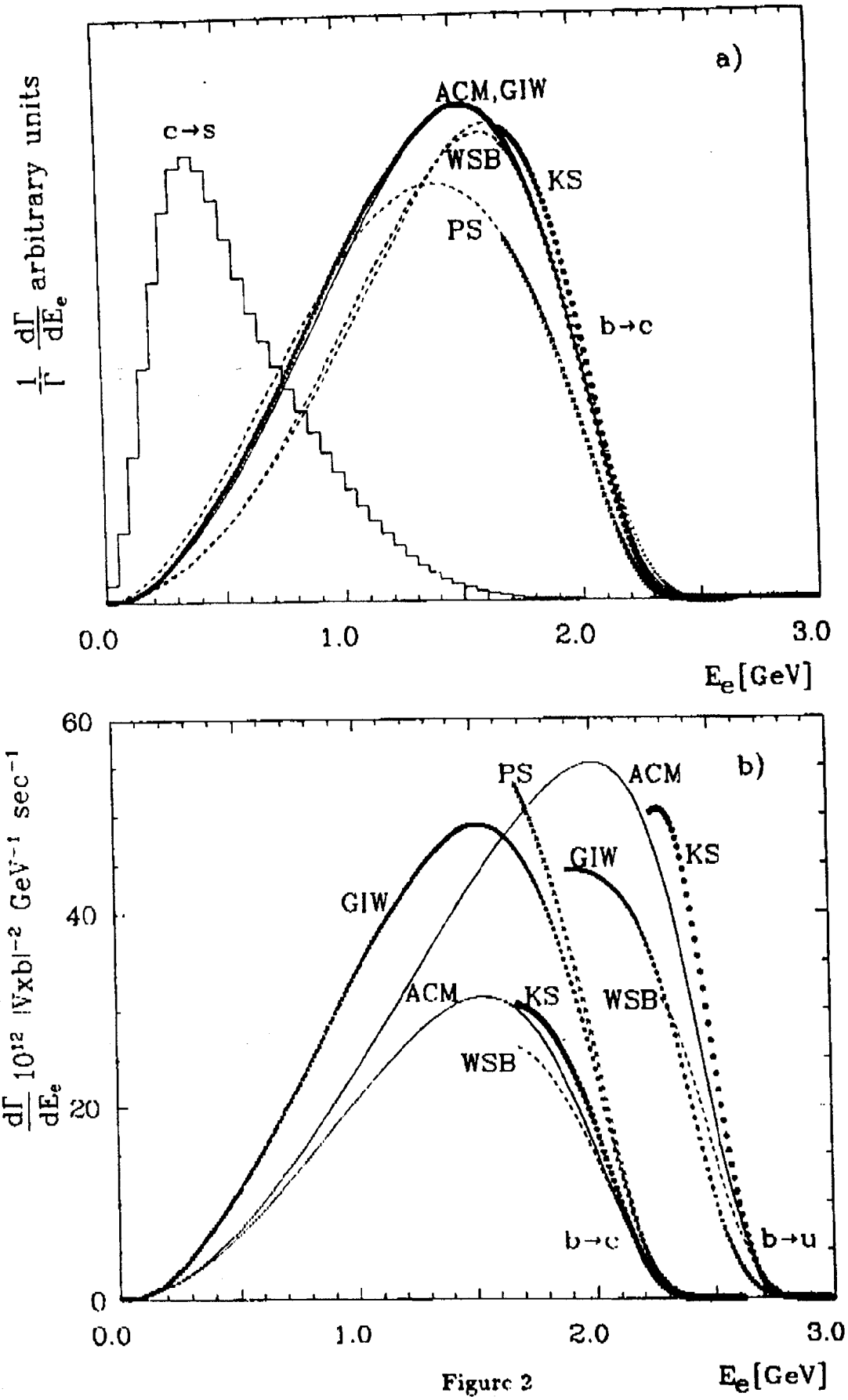
a)
ACM,GIW
c→s
WSB
KS
PS
b→c
$\frac{1}{\Gamma}\frac{d\Gamma}{dE_e}$ arbitrary units
0.0
1.0
2.0
3.0
E_e[GeV]
b)
PS
ACM
GIW
KS
GIW
ACM
KS
WSB
WSB
b→c
b→u
$\frac{d\Gamma}{dE_e}$ 10^{12} $|V_{xb}|^{-2}$ GeV^{-1} sec^{-1}
60
40
20
0
0.0
1.0
2.0
3.0
E_e[GeV]

Figure 2

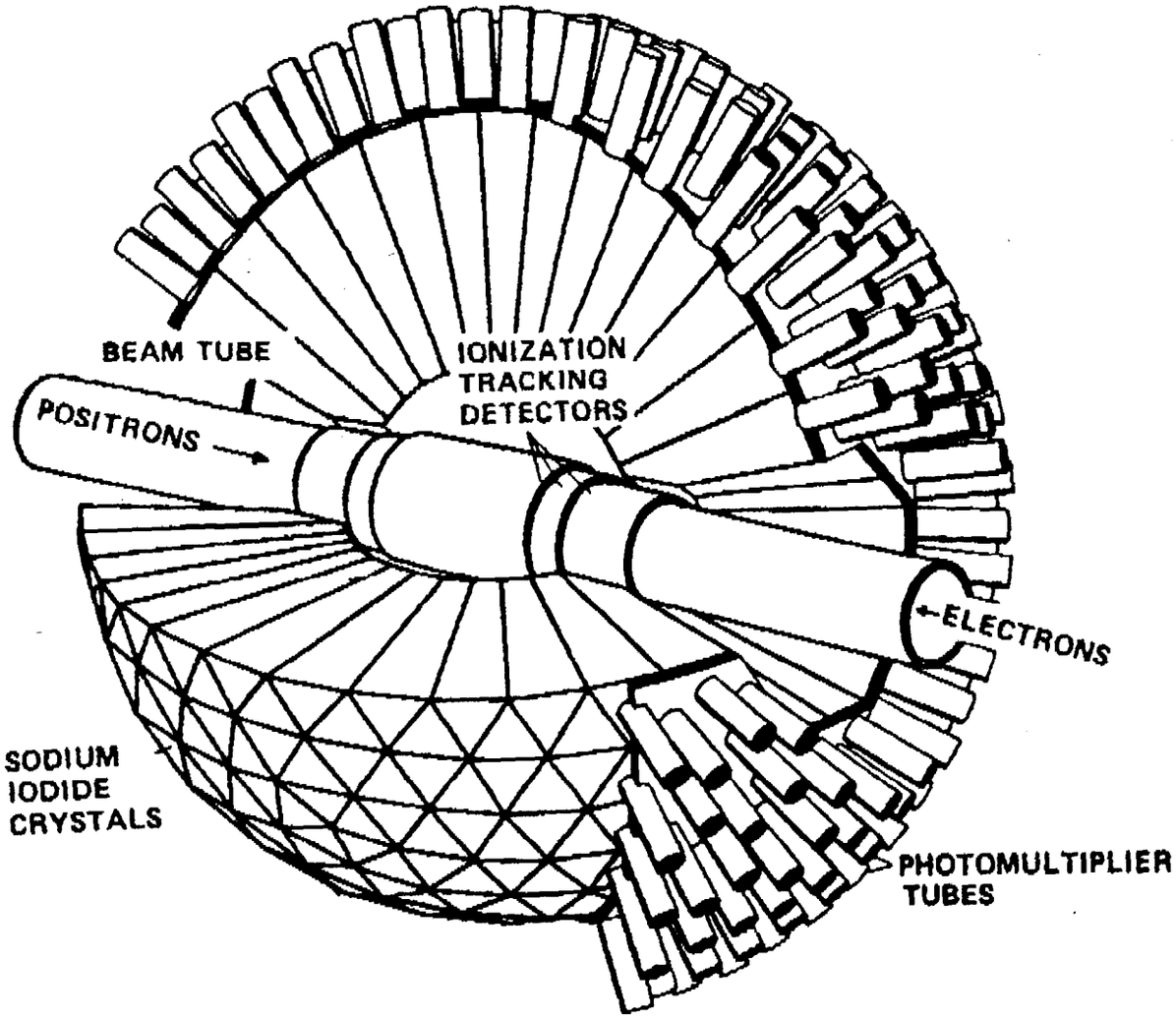
BEAM TUBE
POSITRONS
IONIZATION
TRACKING
DETECTORS
←ELECTRONS
SODIUM
IODIDE
CRYSTALS
PHOTOMULTIPLIER
TUBES

Figure 3

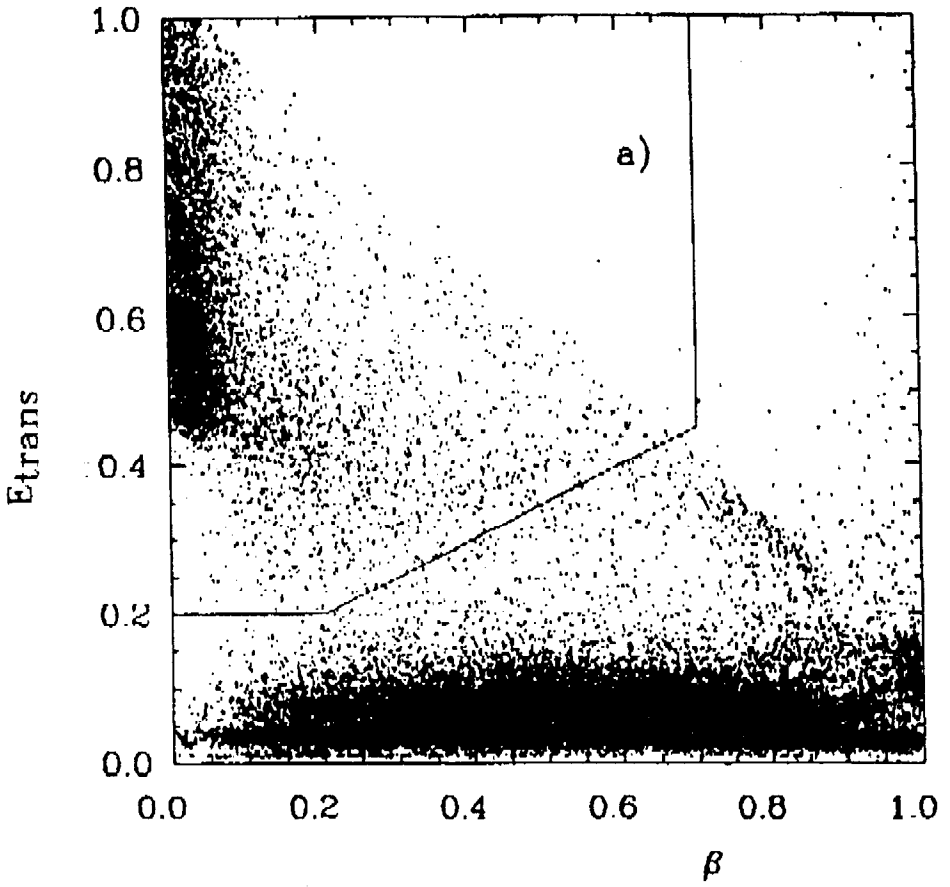
a)
1.0
0.8
0.6
0.4
0.2
0.0
Etrans
0.0
0.2
0.4
0.6
0.8
1.0
β

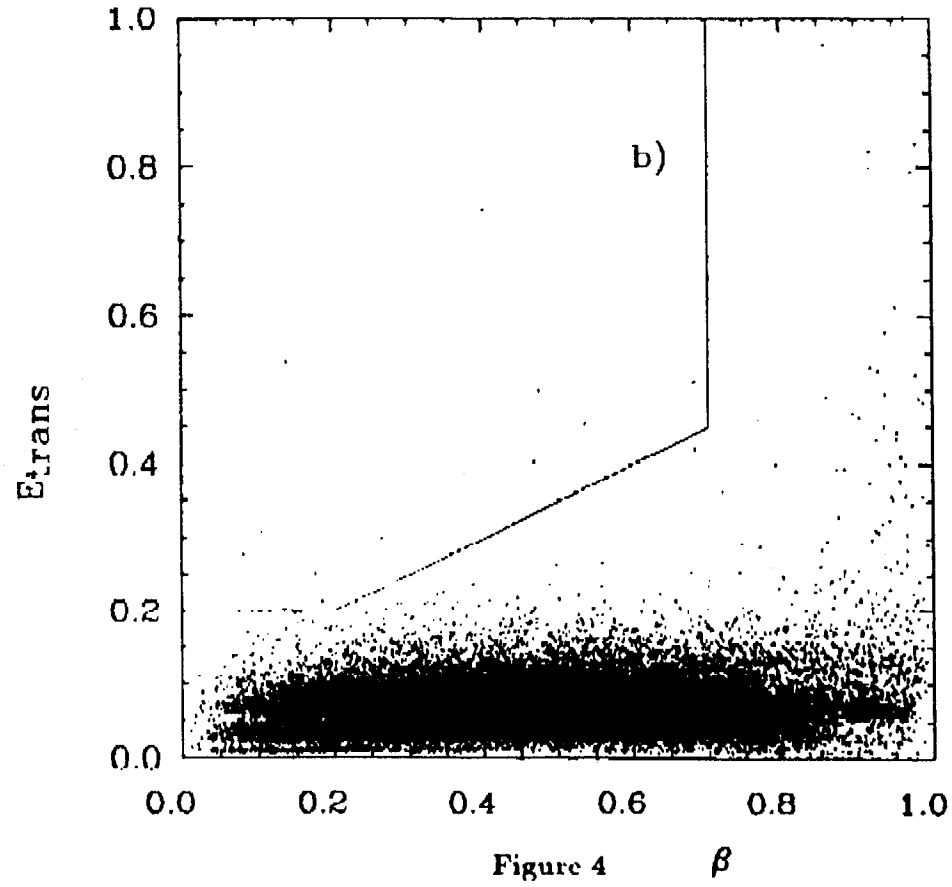
b)
1.0
0.8
0.6
0.4
0.2
0.0
Etrans
0.0
0.2
0.4
0.6
0.8
1.0
β

Figure 4

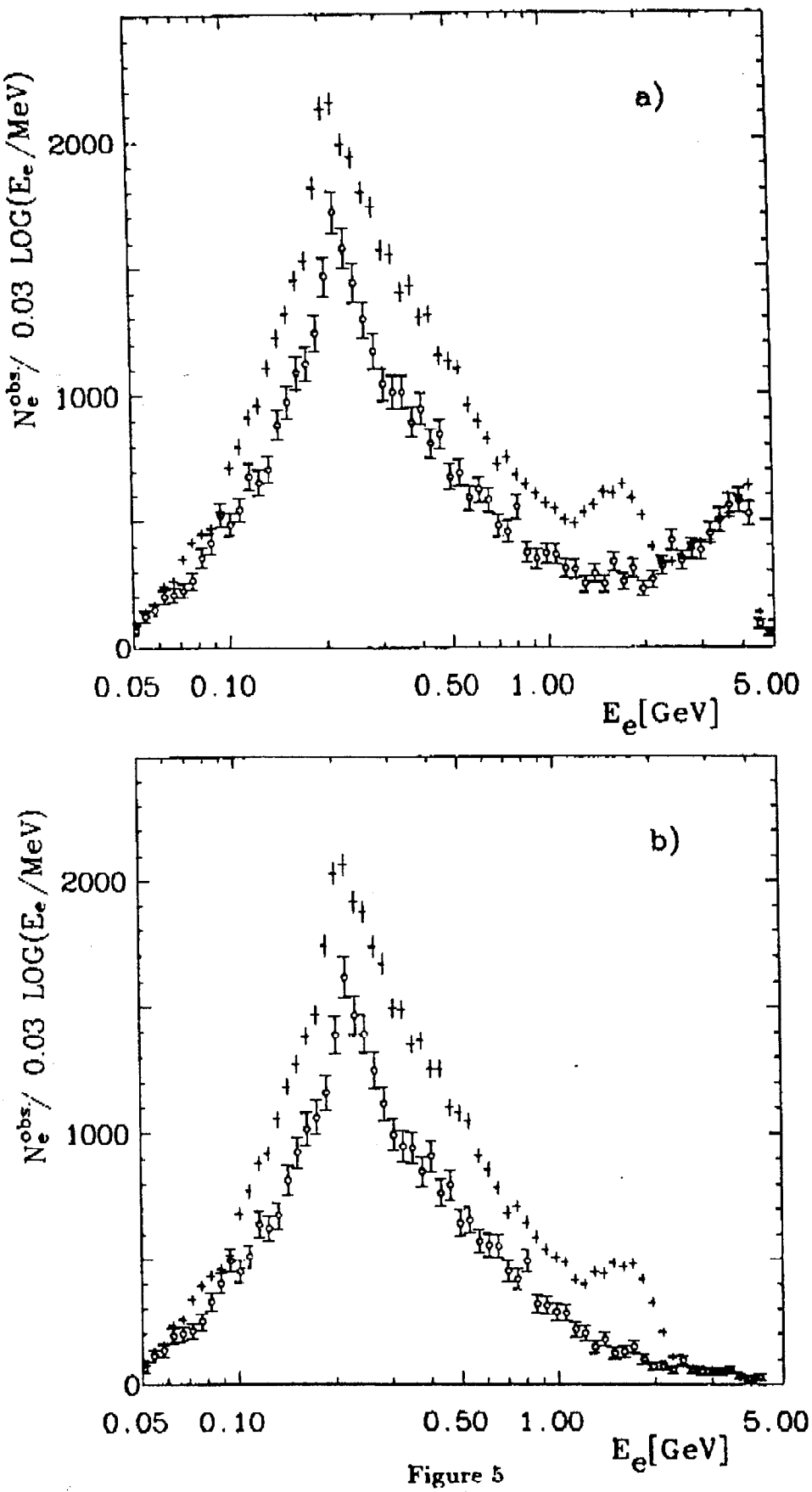

Figure 5

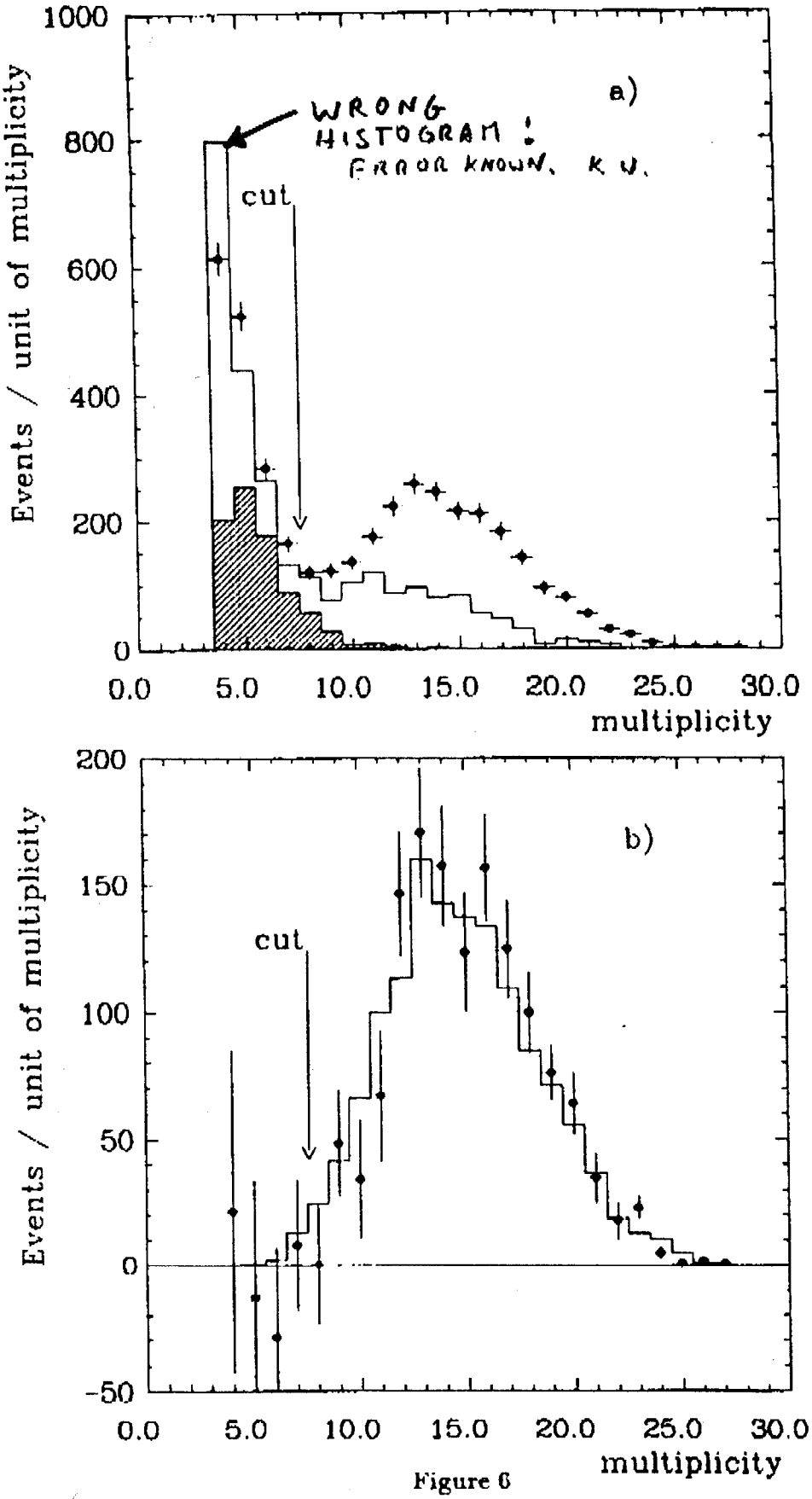
a)
WRONG
HISTOGRAM !
ERROR KNOWN. K.U.
cut
Events / unit of multiplicity
1000
800
600
400
200
0
0.0
5.0
10.0
15.0
20.0
25.0
30.0
multiplicity
b)
cut
Events / unit of multiplicity
200
150
100
50
0
-50
0.0
5.0
10.0
15.0
20.0
25.0
30.0
multiplicity

Figure 6

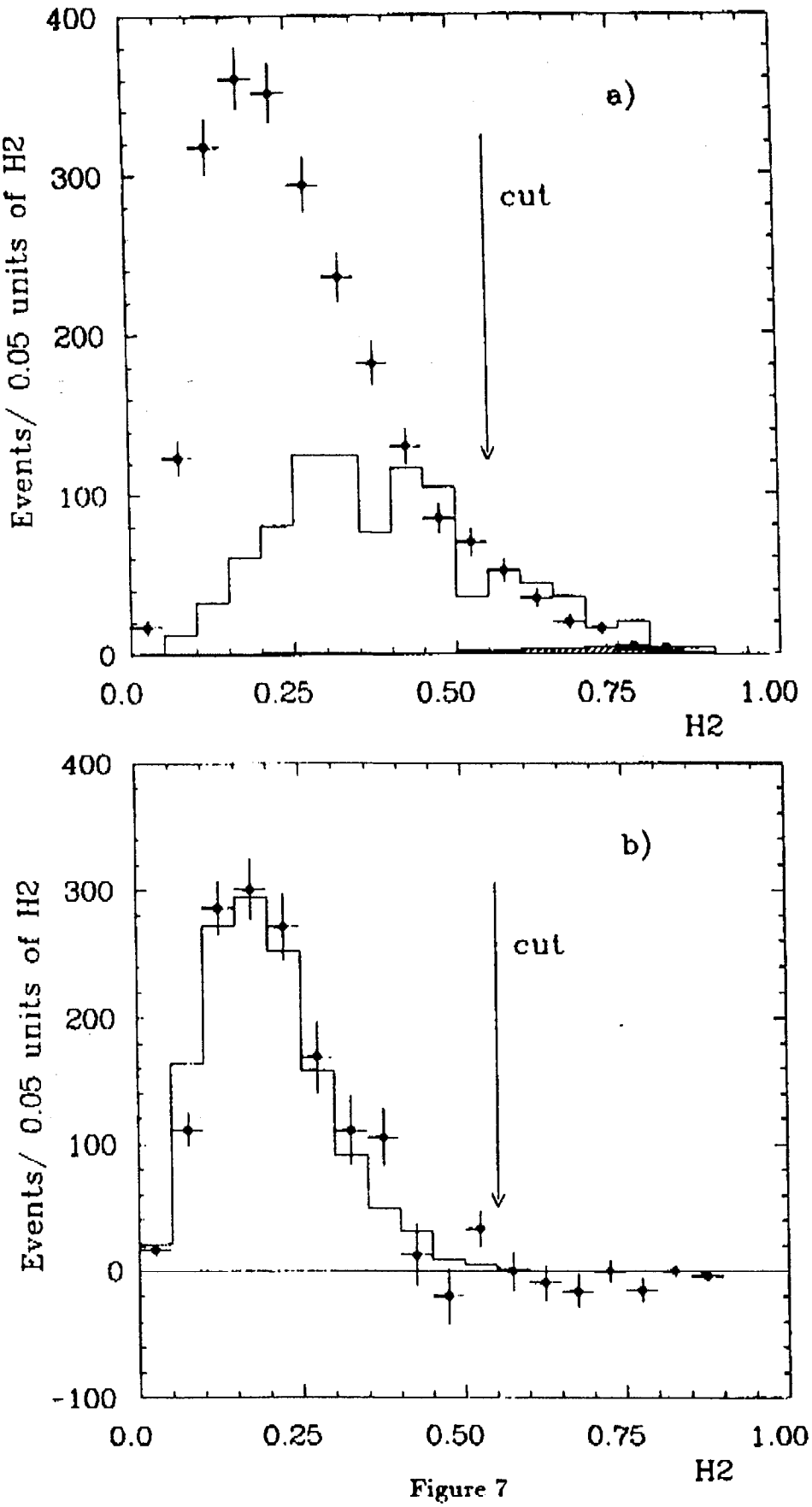
a)
cut
Events/ 0.05 units of H2
400
300
200
100
0
0.0
0.25
0.50
0.75
1.00
H2
b)
cut
Events/ 0.05 units of H2
400
300
200
100
0
-100
0.0
0.25
0.50
0.75
1.00
H2

Figure 7

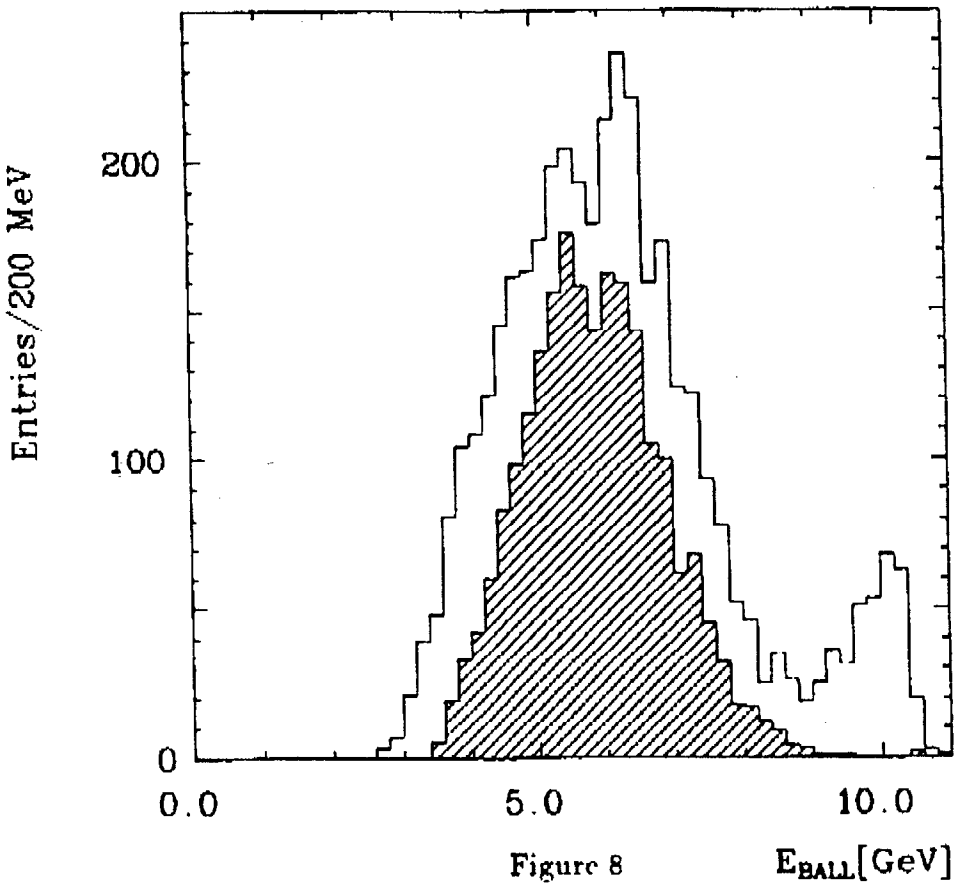

Figure 8

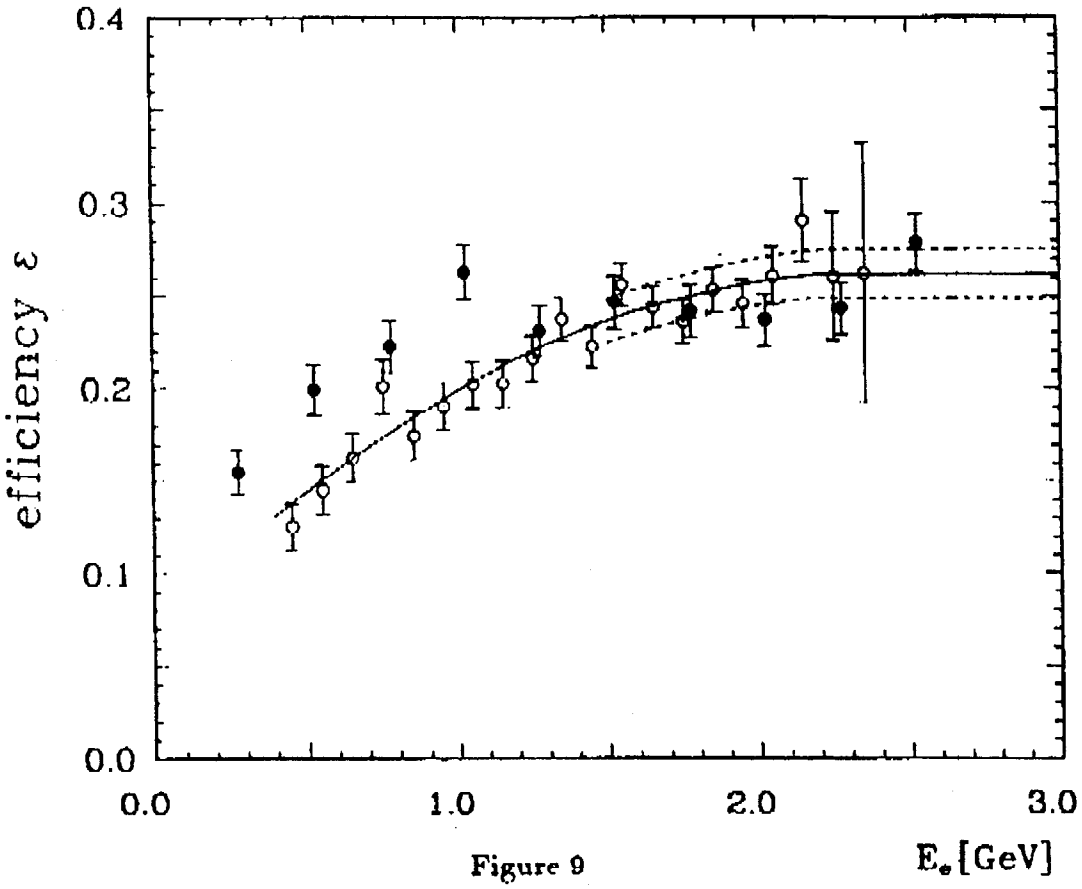

Figure 9

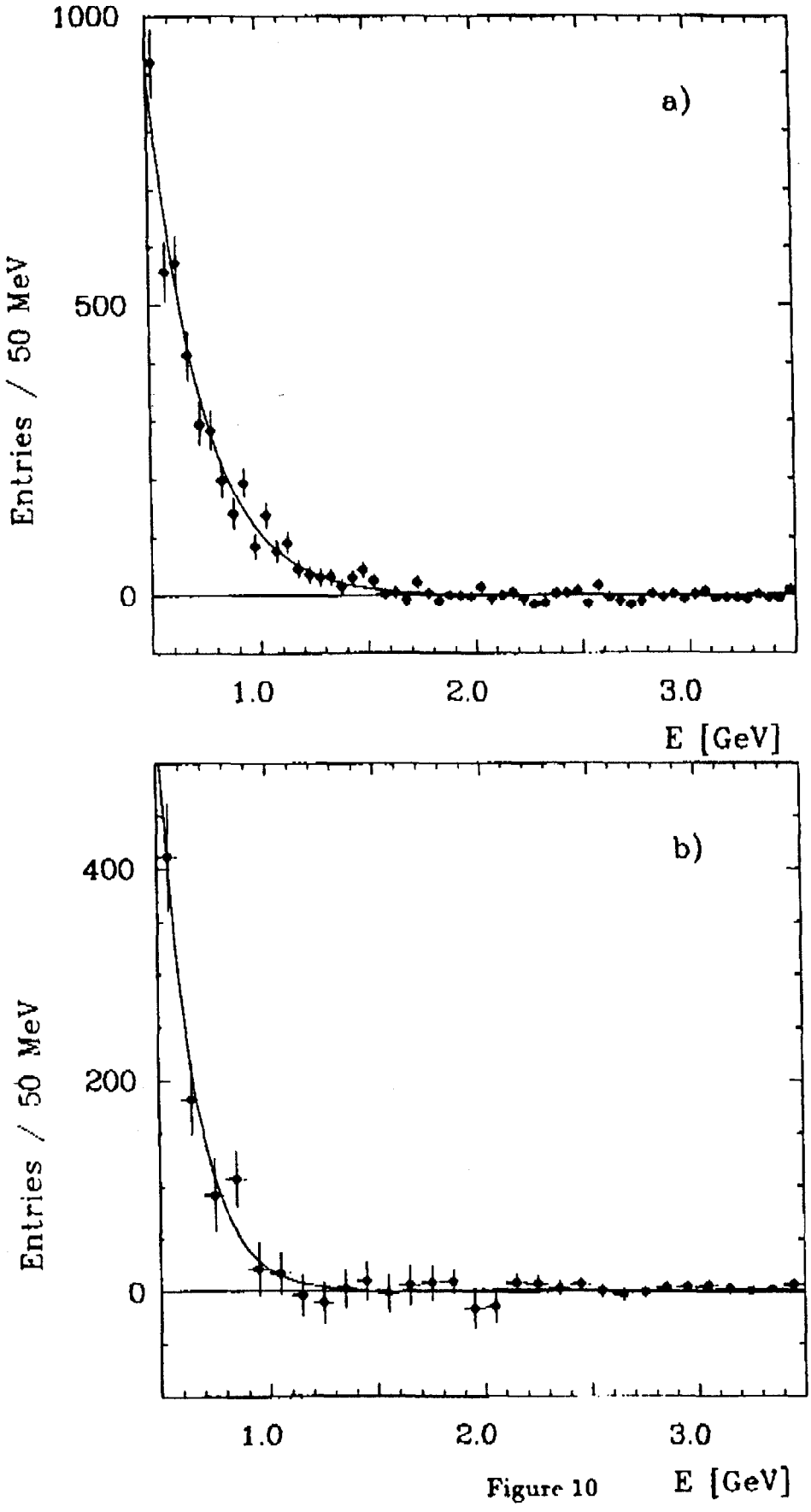
a)
1000
500
0
Entries / 50 MeV
1.0
2.0
3.0
E [GeV]
b)
400
200
0
Entries / 50 MeV
1.0
2.0
3.0
E [GeV]

Figure 10

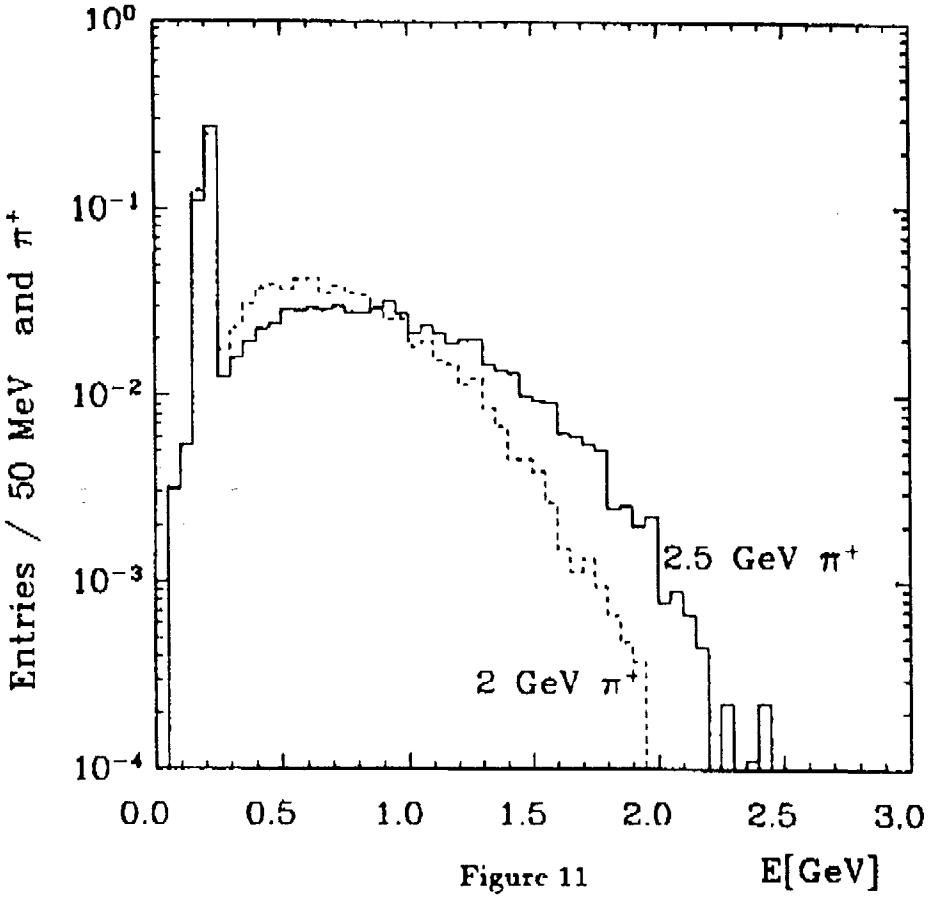

Figure 11

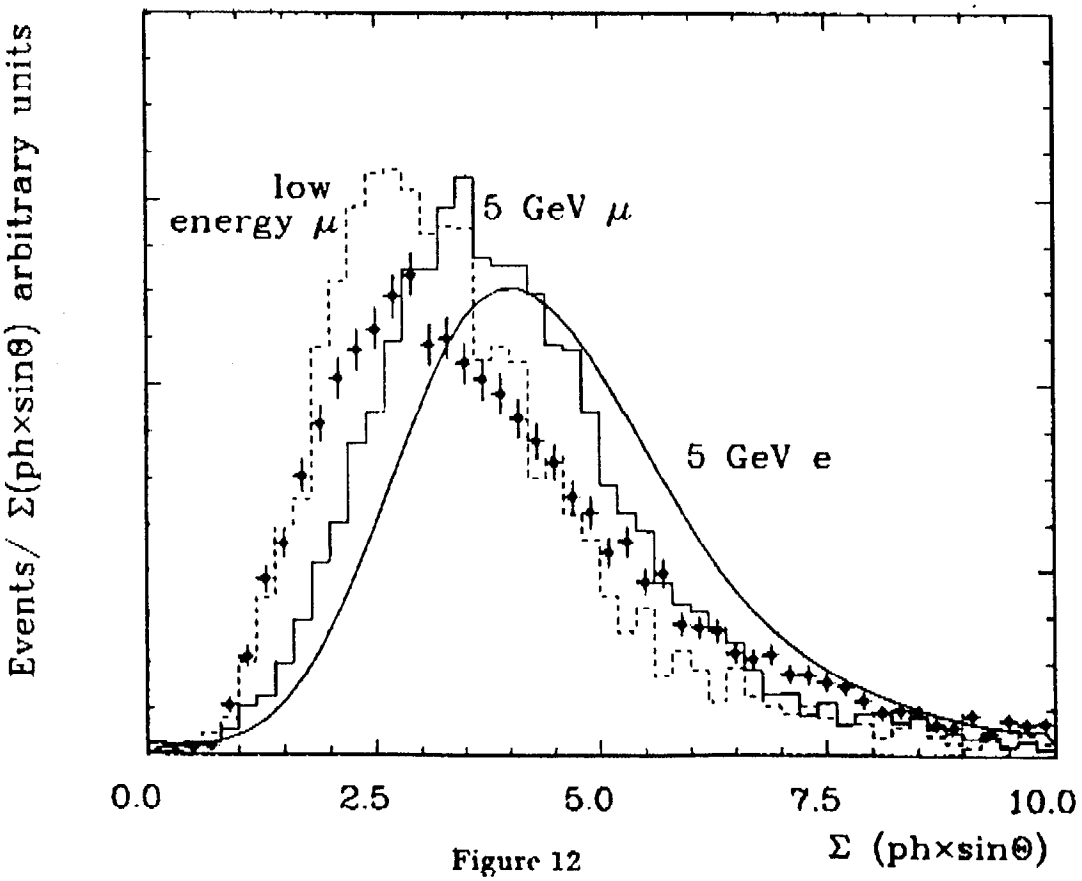

Figure 12

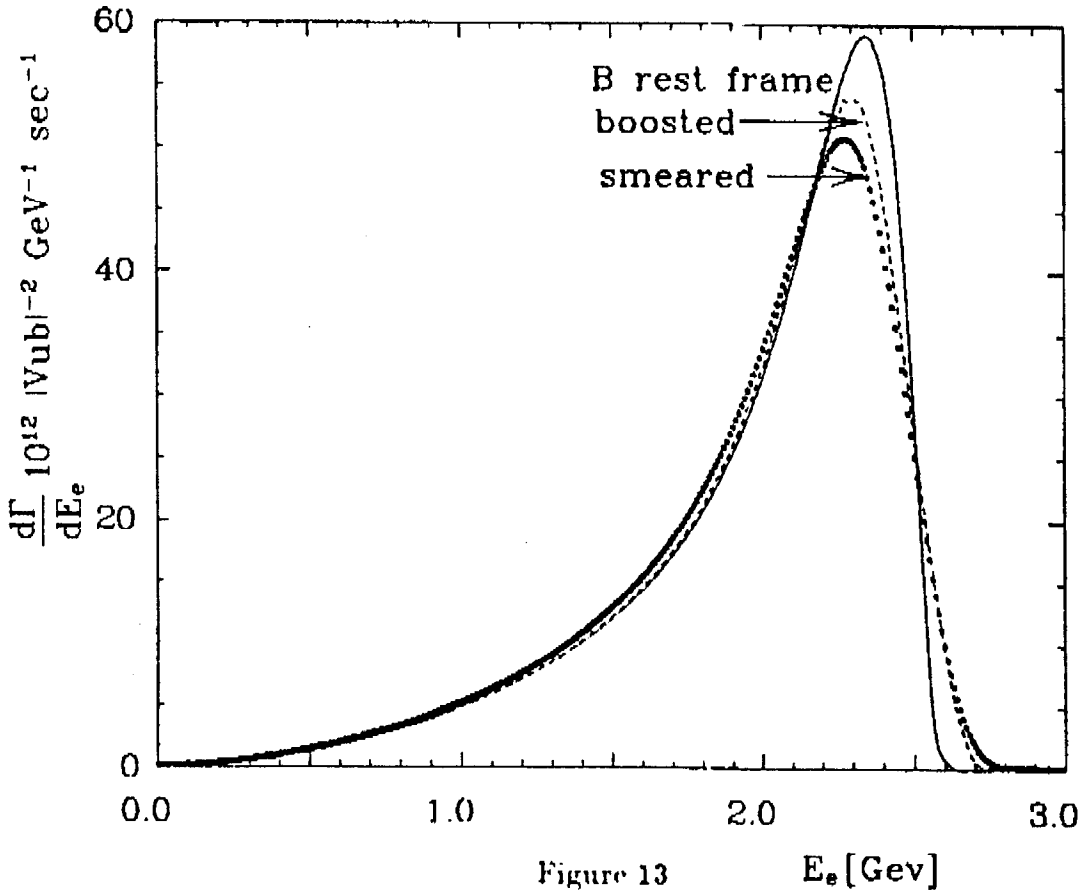
60
40
20
0
0.0
1.0
2.0
3.0
B rest frame
boosted
smeared
$\frac{d\Gamma}{dE_e}\ 10^{12}\ |Vub|^{-2}\ GeV^{-1}\ sec^{-1}$
E_e [Gev]

Figure 13

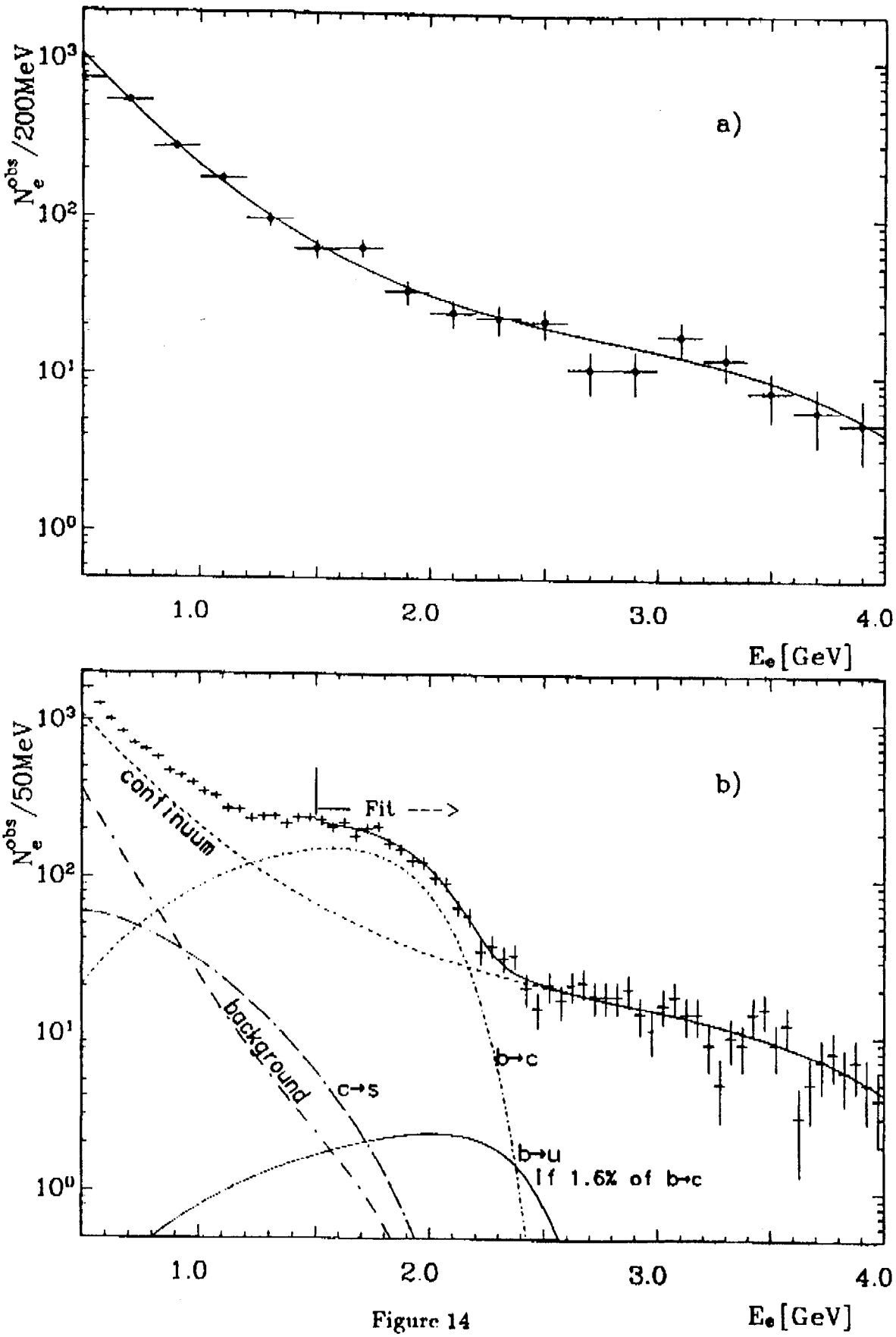
a)
N_e^{obs} /200MeV
10^3
10^2
10^1
10^0
1.0
2.0
3.0
4.0
E_e [GeV]
b)
N_e^{obs} /50MeV
continuum
Fit --->
background
c→s
b→c
b→u
If 1.6% of b→c
10^3
10^2
10^1
10^0
1.0
2.0
3.0
4.0
E_e [GeV]

Figure 14

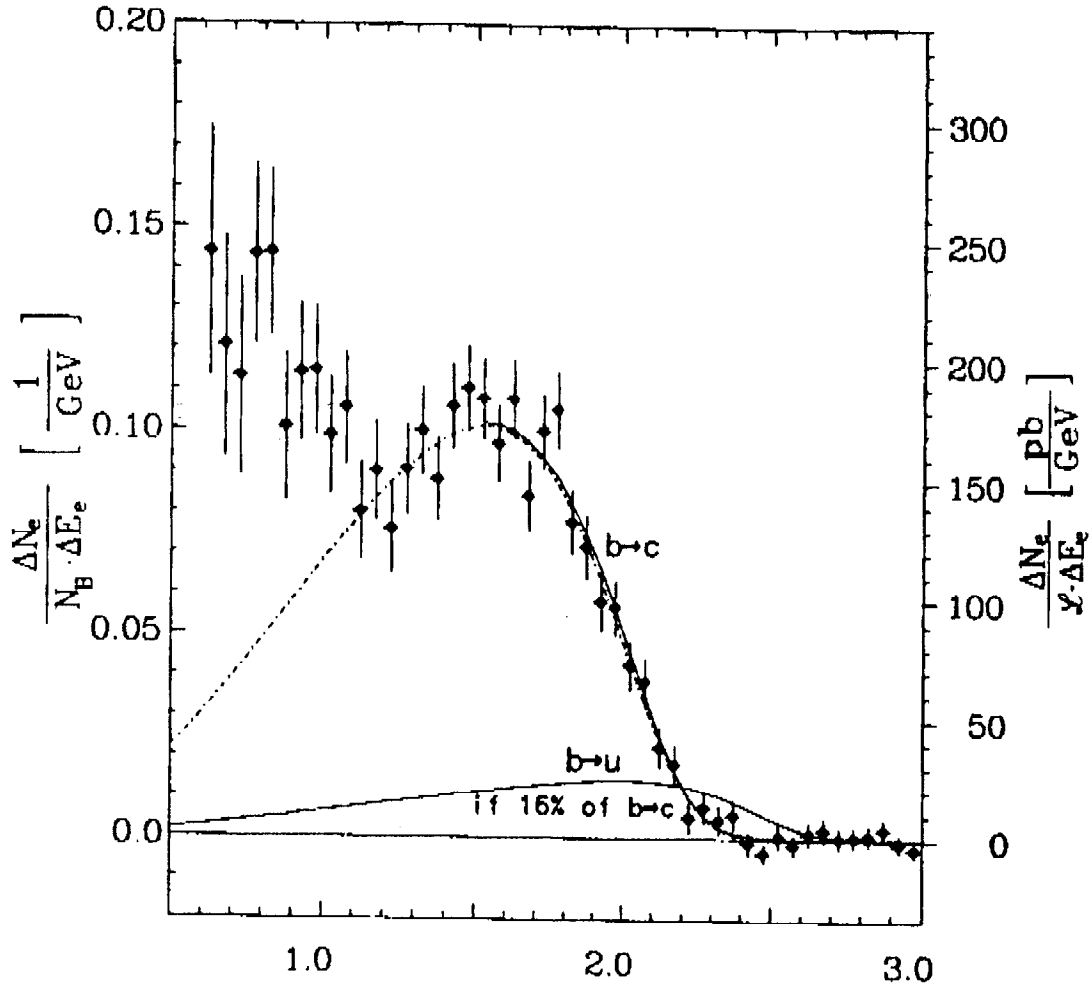

Figure 15

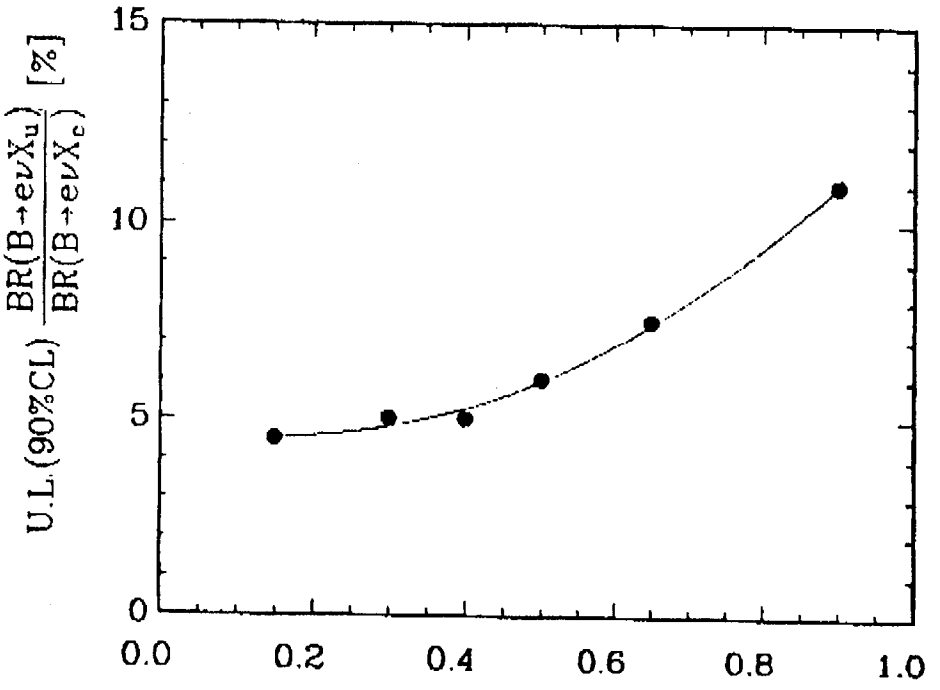

Figure 16

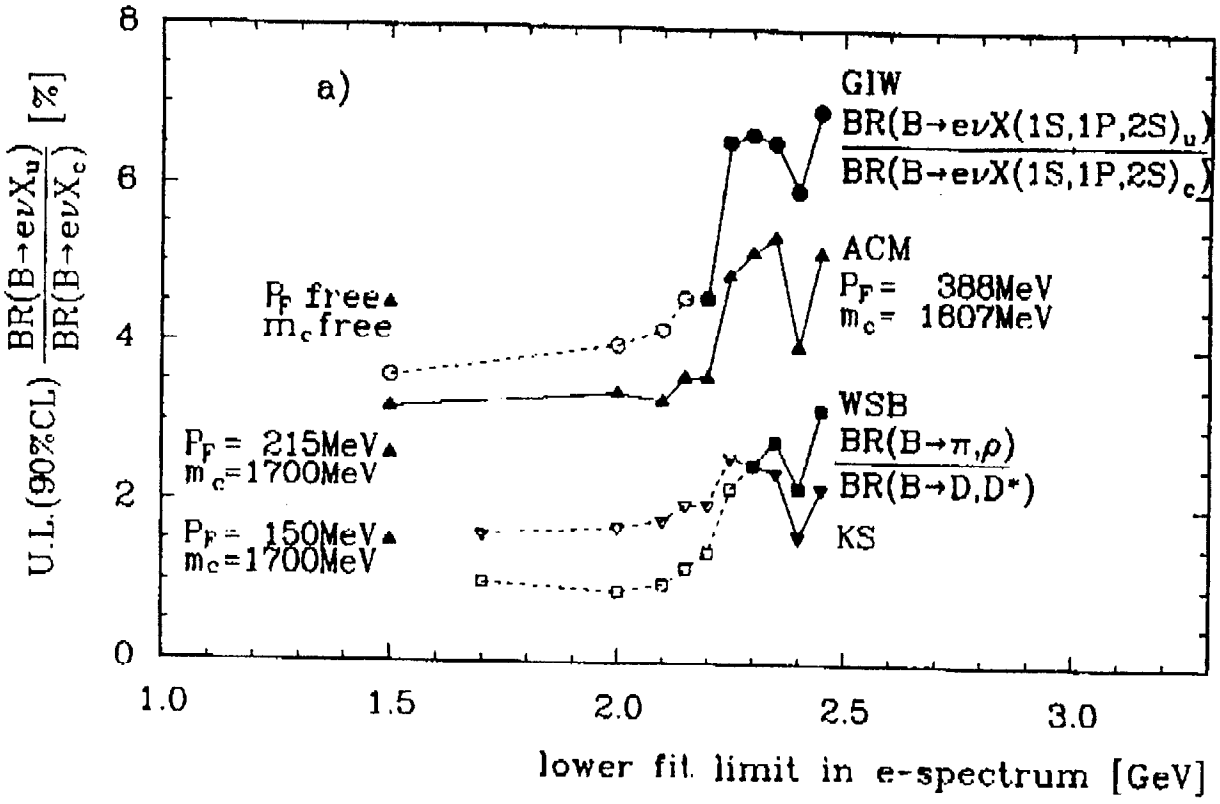

Figure 17

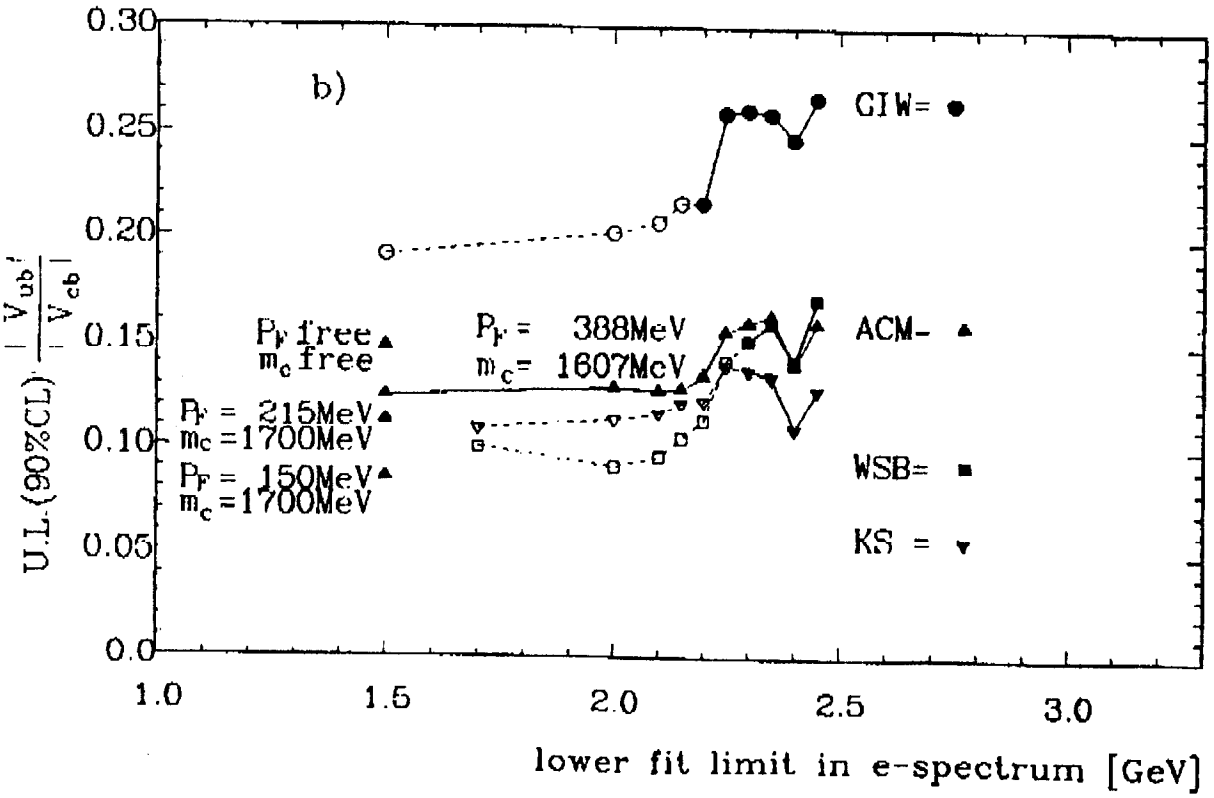

Figure 18